

E. Livanou¹⁰³, A. Lobel²⁶, A. Lorca¹², C. Loup⁴⁴, P. Madrero Pardo¹³, A. Magdaleno Romeo⁷⁸, S. Managau⁶⁶, R.G. Mann⁴⁰, M. Manteiga¹²², J.M. Marchant¹²³, M. Marconi¹¹⁶, J. Marcos³³, M.M.S. Marcos Santos³⁷, D. Marín Pina¹³, S. Marinoni^{51,52}, F. Marocco¹²⁴, D.J. Marshall¹²⁵, L. Martin Polo³⁷, J.M. Martín-Fleitas¹², G. Marton⁵⁸, N. Mary⁶⁶, A. Masip¹³, D. Massari²⁴, A. Mastrobuono-Battisti⁴, T. Mazeh⁹¹, P.J. McMillan¹⁵, S. Messina⁴⁹, D. Michalik³, N.R. Millar⁹, A. Mints⁴⁶, D. Molina¹³, R. Molinaro¹¹⁶, L. Molnár^{58,126,59}, G. Monari⁴⁴, M. Monguió¹³, P. Montegriffo²⁴, A. Montero¹², R. Mor¹³, A. Mora¹², R. Morbidelli²¹, T. Morel³⁸, D. Morris⁴⁰, T. Muraveva²⁴, C.P. Murphy¹¹, I. Musella¹¹⁶, Z. Nagy⁵⁸, L. Noval⁶⁶, F. Ocaña^{33,127}, A. Ogden⁹, C. Ordenovic⁷, J.O. Osinde⁴¹, C. Pagani⁶⁵, I. Pagano⁴⁹, L. Palaversa^{128,9}, P.A. Palicio⁷, L. Pallas-Quintela⁴³, A. Panahi⁹¹, S. Payne-Wardenaar⁶, X. Peñalosa Esteller¹³, A. Penttilä⁵³, B. Pichon⁷, A.M. Piersimoni⁸⁶, F.-X. Pineau⁴⁴, E. Plachy^{58,126,59}, G. Plum⁴, E. Poggio^{7,21}, A. Prša¹²⁹, L. Pulone⁵¹, E. Racero^{37,127}, S. Ragaini²⁴, M. Rainer^{19,130}, C.M. Raiteri²¹, N. Rambaux³⁶, P. Ramos^{13,44}, M. Ramos-Lerate³³, P. Re Fiorentin²¹, S. Regibo⁶⁰, P.J. Richards¹³¹, C. Rios Diaz⁴¹, V. Ripepi¹¹⁶, A. Riva²¹, H.-W. Rix²⁰, G. Rixon⁹, N. Robichon⁴, A.C. Robin⁵⁵, C. Robin⁶⁶, M. Roelens¹⁰, H.R.O. Rogues⁸⁸, L. Rohrbasser³⁰, M. Romero-Gómez¹³, N. Rowell⁴⁰, F. Royer⁴, D. Ruz Mieres⁹, K.A. Rybicki¹¹³, G. Sadowski¹⁷, A. Sáez Núñez¹³, A. Sagristà Sellés⁶, J. Sahlmann⁴¹, E. Salguero⁴², N. Samaras^{26,132}, V. Sanchez Gimenez¹³, N. Sanna¹⁹, R. Santoveña⁴³, M. Sarasso²¹, M. Schultheis⁷, E. Sciacca⁴⁹, M. Segol⁸⁸, J.C. Segovia³⁷, D. Ségransan¹⁰, D. Semeux⁷³, S. Shahaf¹³³, H.I. Siddiqui¹³⁴, A. Siebert^{44,93}, L. Siltala⁵³, A. Silvelo⁴³, E. Slezak⁷, I. Slezak⁷, R.L. Smart²¹, O.N. Snaith⁴, E. Solano¹³⁵, F. Solitro²⁸, D. Souami^{111,136}, J. Souchay³⁴, A. Spagna²¹, L. Spina¹, F. Spoto⁷², I.A. Steele¹²³, H. Steidelmüller¹⁴, C.A. Stephenson^{33,137}, M. Süveges¹³⁸, J. Surdej^{38,139}, L. Szabados⁵⁸, E. Szegedi-Elek⁵⁸, F. Taris³⁴, M.B. Taylor¹⁴⁰, R. Teixeira⁸⁷, L. Tolomei²⁸, N. Tonello⁹⁹, F. Torra²⁵, J. Torra¹³, G. Torralba Elipe⁴³, M. Trabucchi^{141,10}, A.T. Tsounis¹⁴², C. Turon⁴, A. Ulla¹⁴³, N. Unger¹⁰, M.V. Vaillant⁶⁶, E. van Dillen⁸⁸, W. van Reeve¹⁴⁴, O. Vanel⁴, A. Vecchiato²¹, Y. Viala⁴, D. Vicente⁹⁹, S. Voutsinas⁴⁰, M. Weiler¹³, T. Wevers^{9,145}, Ł. Wyrzykowski¹¹³, A. Yoldas⁹, P. Yvard⁸⁸, H. Zhao⁷, J. Zorec¹⁴⁶, S. Zucker⁷¹, and T. Zwitter¹⁴⁷

(Affiliations can be found after the references)

Received May 3, 2022 ; accepted June 1st, 2022

ABSTRACT

Context. We present the third data release of the European Space Agency’s *Gaia* mission, *Gaia* DR3. This release includes a large variety of new data products, notably a much expanded radial velocity survey and a very extensive astrophysical characterisation of *Gaia* sources.

Aims. We outline the content and the properties of *Gaia* DR3, providing an overview of the main improvements in the data processing in comparison with previous data releases (where applicable) and a brief discussion of the limitations of the data in this release.

Methods. The *Gaia* DR3 catalogue is the outcome of the processing of raw data collected with the *Gaia* instruments during the first 34 months of the mission by the *Gaia* Data Processing and Analysis Consortium.

Results. The *Gaia* DR3 catalogue contains the same source list, celestial positions, proper motions, parallaxes, and broad band photometry in the G , G_{BP} , and G_{RP} pass-bands already present in the Early Third Data Release, *Gaia* EDR3. *Gaia* DR3 introduces an impressive wealth of new data products. More than 33 million objects in the ranges $G_{RVS} < 14$ and $3100 < T_{\text{eff}} < 14500$, have new determinations of their mean radial velocities based on data collected by *Gaia*. We provide G_{RVS} magnitudes for most sources with radial velocities, and a line broadening parameter is listed for a subset of these. Mean *Gaia* spectra are made available to the community. The *Gaia* DR3 catalogue includes about 1 million mean spectra from the radial velocity spectrometer, and about 220 million low-resolution blue and red prism photometer BP/RP mean spectra. The results of the analysis of epoch photometry are provided for some 10 million sources across 24 variability types. *Gaia* DR3 includes astrophysical parameters and source class probabilities for about 470 million and 1500 million sources, respectively, including stars, galaxies, and quasars. Orbital elements and trend parameters are provided for some 800 000 astrometric, spectroscopic and eclipsing binaries. More than 150 000 Solar System objects, including new discoveries, with preliminary orbital solutions and individual epoch observations are part of this release. Reflectance spectra derived from the epoch BP/RP spectral data are published for about 60 000 asteroids. Finally, an additional data set is provided, namely the *Gaia* Andromeda Photometric Survey, consisting of the photometric time series for all sources located in a 5.5 degree radius field centred on the Andromeda galaxy.

Conclusions. This data release represents a major advance with respect to *Gaia* DR2 and *Gaia* EDR3 because of the unprecedented quantity, quality, and variety of source astrophysical data. To date this is the largest collection of all-sky spectrophotometry, radial velocities, variables, and astrophysical parameters derived from both low- and high-resolution spectra and includes a spectrophotometric and dynamical survey of SSOs of the highest accuracy. The non-single star content surpasses the existing data by orders of magnitude. The quasar host and galaxy light profile collection is the first such survey that is all sky and space based. The astrophysical information provided in *Gaia* DR3 will unleash the full potential of *Gaia*’s exquisite astrometric, photometric, and radial velocity surveys.

Key words. catalogs - astrometry - parallaxes - proper motions - techniques: photometric - techniques: radial velocities - techniques: spectroscopic

1. Introduction

The European Space Agency’s (ESA) *Gaia* mission (Gaia Collaboration, Prusti et al. 2016), launched in 2013, is now at its

third data release (*Gaia* DR3). The aim of this paper is to present the *Gaia* DR3 data products, providing a brief overview of the new features introduced in the processing and discussing the quality of the data. *Gaia* EDR3 (Gaia Collaboration, Brown et al. 2021) was the first instalment of the full *Gaia* DR3 and included astrometry and broad band photometry for a total of 1.8 billion objects based on 34 months of satellite operations. Radial velocities for 7 million sources were copied over from the second data release, *Gaia* DR2, where a small number of spurious radial velocities were removed (Seabroke et al. 2021).

Gaia DR3 complements *Gaia* EDR3, introducing a vast array of new data products based on the same source catalogue and raw observations at the basis of *Gaia* EDR3. Indeed, the astrometry and broad band photometry in G , G_{BP} , and G_{RP} from *Gaia* EDR3 are repeated in the new catalogue (but see section 3.1 for G correction). New data products in *Gaia* DR3 include mean low-resolution blue and red photometer (BP/RP) spectra and high-resolution Radial Velocity Spectrometer (RVS) spectra; new estimates of mean radial velocities to a fainter limiting magnitude; line broadening and chemical composition information derived from RVS spectra; variable-star classification and characterisation; and photometric time series for over 20 classes of variables. Photometric time series for all sources, variable and non-variable, are available for a field centred on the Andromeda galaxy. A large sample of Solar System objects (SSOs) with orbital solutions and epoch observations is part of the data release, together with reflectance spectra for a subset of those. *Gaia* DR3 also includes results for non-single stars (NSS), quasars, and galaxies. For a large fraction of the objects, the catalogue lists astrophysical parameters (APs) determined from parallaxes, broad band photometry, and the mean RVS or mean BP/RP spectra.

To enhance the scientific exploitation of the data, the *Gaia* archive includes pre-computed cross-matches with selected external optical and near-infrared photometric and spectroscopic surveys. In addition to the catalogues described in Gaia Collaboration, Brown et al. (2021), *Gaia* DR3 includes the sixth data release from the Radial Velocity Experiment (RAVE) survey (Steinmetz et al. 2020a). The *Gaia* Universe Model Snapshot (GUMS, version 20, Robin et al. 2012) and the corresponding simulated *Gaia* catalogue (GOG) were also already included in *Gaia* EDR3. The details on these supplementary data can be found in the online documentation¹.

This paper is organised as follows. Section 2 summarises the *Gaia* instruments and their wavelength ranges; section 3 summarises the properties of the astrometric and photometric data already included in *Gaia* EDR3; section 4 presents the BP/RP spectra; section 5 outlines the RVS data processing, listing the improvements implemented in *Gaia* DR3, and presents the new RVS data products, the line broadening velocity (v_{broad}) and the G_{RVS} magnitude. Section 6 deals with the variable source content of the catalogue including the *Gaia* Andromeda Photometric Survey (GAPS); section 7 discusses the NSS content of the release; section 8 comments on the SSOs; section 9 provides information about the APs; section 10 presents the extended object (EO) data processing and results. Section 11 describes the extragalactic content of *Gaia* DR3, that is, information on galaxies and quasi-stellar objects (QSOs) or ‘quasars’ derived by several data processing modules. Section 12 comments on the quality of the release and section 13 provides references to the software

tools that are offered to the users to deal with *Gaia* DR3 data. Finally, section 14 presents some concluding remarks.

Each data product section briefly summarises the main limitations of the data, and makes reference to the relevant *Gaia* Collaboration and *Gaia* Data Processing and Analysis Consortium (DPAC) papers where more details can be found. For a number of technical details, we refer the reader to the online documentation.

All the papers accompanying *Gaia* DR3 are published in the Astronomy & Astrophysics special issue on *Gaia* DR3. Finally, we recall that all the *Gaia* data releases are made available through the archive hosted by ESA², as described in Gaia Collaboration, Brown et al. (2021) and references therein. Partner and affiliated data centres in Europe, the United States, Japan, Australia, and South Africa provide access to the data through their own facilities.

2. Data processing

The *Gaia* satellite has three main instruments on board: the astrometric instrument collecting images in *Gaia*’s white-light G -band (330–1050 nm), the blue BP and red RP prism photometers for low-resolution spectra, and, finally, the RVS. BP/RP spectral data cover the wavelength ranges 330–680 nm and 640–1050 nm, respectively. The resolution is variable and ranges from 30 to 100 for BP and 70 to 100 for RP in $\lambda/\Delta\lambda$, depending on the position in the spectrum and on the CCD (see Carasco et al. 2021). In the RVS spectra, the starlight is dispersed over about 1100 pixels in the *Gaia* telescopes scanning direction (along-scan, AL), sampling the wavelength range from 845 to 872 nm. The resolving power is $R \sim 11\,500$ (with a resolution element of about 3 pixels). As the wings of the spectra are excluded from the processing, the effective wavelength range of the processed spectra is reduced to 846–870 nm (Sartoretti et al. 2022a). Similarly to *Gaia* EDR3, *Gaia* DR3 is based on data collected over a 34-month time interval (for details see Gaia Collaboration, Brown et al. 2021). The *Gaia* data processing is the responsibility of DPAC and is presented in Gaia Collaboration, Prusti et al. (2016).

The basic statistics on the source numbers for each of the data products in *Gaia* DR3 can be found in Table 1, with further details in Table 2. The categories listed in the tables are described in the text below. A visual impression of the release contents is given in Fig. 1 which shows histograms of the distribution in G of the main categories of data products in *Gaia* DR3.

3. Astrometry and broad band photometry

The astrometric and broad band photometry content of *Gaia* DR3 is the same as that for *Gaia* EDR3, except for the addition of the G_{RVS} photometry, but for convenience we summarise here the properties of these data products. *Gaia* EDR3 provided celestial positions and the apparent brightness in G for 1.8 billion sources. For 1.5 billion of those sources, parallaxes, proper motions, and the $(G_{BP} - G_{RP})$ colour were also published. *Gaia* DR3 therefore contains some 585 million sources with five-parameter astrometry (two positions, the parallax, and two proper motion components), and about 882 million sources with six-parameter (6-p) astrometry, including an additional pseudo-colour parameter. We refer to Gaia Collaboration, Brown et al. (2021) for details on *Gaia* EDR3, a summary of the astrometric

¹ *Gaia* DR3 online documentation: <https://www.cosmos.esa.int/web/gaia-users/archive/gdr3-documentation>

² <https://archives.esac.esa.int/gaia>

Table 1. Number of sources of a certain type, or the number of sources for which a given data product is available in *Gaia* DR3.

Data product or source type	Number of sources	Comments
Total	1 811 709 771	
5-parameter astrometry	585 416 709	
6-parameter astrometry	882 328 109	
2-parameter astrometry	343 964 953	
<i>Gaia</i> -CRF3 sources	1 614 173	
ICRF3 sources used for frame orientation	2007	
<i>Gaia</i> -CRF3 sources used for frame spin	428 034	
<i>G</i> -band	1 806 254 432	
<i>G</i> _{BP} -band	1 542 033 472	
<i>G</i> _{RP} -band	1 554 997 939	
Photometric time series	11 754 237	
Gaia Andromeda Photometric Survey	1 257 319	Photometric time series for all sources in 5.5° radius field around M31
Radial velocity	33 812 183	$G_{RVS} < 14$, $3100 < T_{\text{eff}} < 14\,500$ K
<i>G</i> _{RVS} -band	32 232 187	
v_{broad}	3 524 677	spectral line broadening parameter
Radial velocity time series	1898	Sample of Cepheids and RR Lyrae
BP/RP mean spectra	219 197 643	$G < 17.65$ with small number of exceptions
RVS mean spectra	999 645	AFGK spectral types with SNR > 20, and sample of lower SNR spectra
Variable sources	10 509 536	See Table 2
Object DSC classification	1 590 760 469	
Self-organised map of poorly classified sources	1	30 × 30 map and prototype spectra
APs from mean BP/RP spectra	470 759 263	$G < 19$, see Table 2
APs from mean RVS spectra	5 591 594	
Chemical abundances from mean RVS spectra	2 513 593	Up to 12 elements
DIBs from mean RVS spectra	472 584	
Non-single stars	813 687	astrometric, spectroscopic, eclipsing, orbits, trends, see Table 2
QSO candidates	6 649 162	High completeness, low purity
QSO redshifts	6 375 063	
QSO host galaxy detected	64 498	
QSO host galaxy profile	15 867	
Galaxy candidates	4 842 342	High completeness, low purity
Galaxy redshifts	1 367 153	
Galaxy profiles	914 837	
Solar System objects	158 152	Epoch astrometry and photometry
SSO reflectance spectra	60 518	
Total galactic extinction maps	5	HEALPix levels 6–9, and optimum HEALPix level
Science alerts	2612	Triggered in the period 25-07-2014 to 28-05-2017

Table 2. Further details on the number of sources of a certain type, or the number of sources for which a given data product is available in *Gaia* DR3.

Data product or source type	Number of sources	Comments
Variable sources		
Total	10 509 536	
Classified with supervised machine learning	9 976 881	24 variability types or type groups
Active galactic nuclei	872 228	
Cepheids	15 021	
Compact companions	6 306	
Eclipsing binaries	2 184 477	
Long-period variables	1 720 588	
Microlensing events	363	
Planetary transits	214	
RR Lyrae stars	271 779	
Short-timescale variables	471 679	
Solar-like rotational modulation variables	474 026	
Upper-main-sequence oscillators	54 476	
Astrophysical parameters from mean BP/RP spectra		
Total	470 759 263	$G < 19$
Spectroscopic parameters	470 759 263	
Interstellar extinction and distances	470 759 263	
MCMC samples from the BP/RP AP estimation	449 297 716	
APs assuming an unresolved binary	348 711 151	
MCMC samples from BP/RP unresolved binary AP estimation	348 711 151	
Evolutionary parameters	128 611 111	mass, age, evolutionary stage
Stars with emission-line classifications	57 511	
Sources with spectral types	217 982 837	
Hot stars with spectroscopic parameters	2 382 015	
Ultra-cool stars	94 158	
Cool stars with activity index	1 349 499	
Sources with $H\alpha$ emission measurements	235 384 119	
Non-single stars		
Total	813 687	
Acceleration solutions	338 215	
Orbital astrometric solutions	169 227	including astroSpectroSB1 combined solutions
Orbital spectroscopic solutions (SB1/SB2)	220 372	including astroSpectroSB1 combined solutions
Trend spectroscopic solutions	56 808	
Eclipsing binaries	87 073	including eclipsingSpectro combined solutions

and photometric data processing, and a summary of the limitations of these data and guidance on their use. Detailed descriptions of the astrometry in *Gaia* EDR3 (and thus also *Gaia* DR3) are provided in [Lindegren et al. \(2021b\)](#), while the broad band photometry is described in detail in [Riello et al. \(2021\)](#). Details

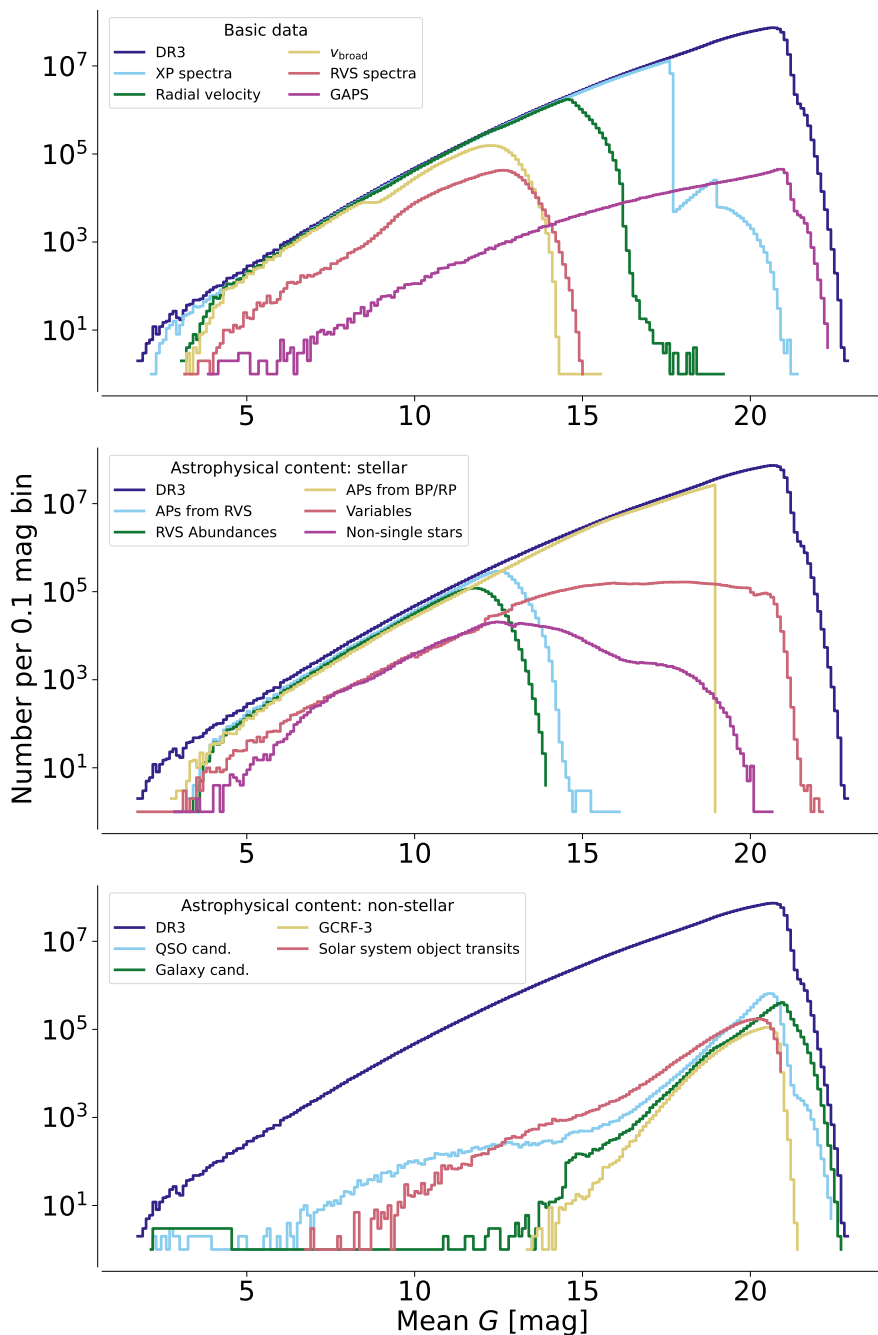


Fig. 1. Distribution of the mean values of G for the main *Gaia* DR3 components shown as histograms with bins of 0.1 mag in width. The top panel shows the histograms for the basic observational data in *Gaia* DR3 (spectra, radial velocities, v_{broad} , photometric time series). The middle panel shows histograms for the stellar astrophysical contents, and the bottom panel shows the non-stellar astrophysical contents. The sharp transitions in the top and middle panels at $G = 17.65$ and $G = 19$ are caused by the limit on the brightness of sources for which BP/RP spectra are published and the limit up to which astrophysical parameters were estimated. The SSO histogram shows the distribution of the transit-level G -band magnitudes (see Tanga et al. 2022, for a distribution of solar system objects in absolute magnitude H). The QSO and galaxy candidate histograms extend to very bright magnitudes which is a consequence of favouring completeness over purity in these samples, and not applying any filtering to remove them (see Gaia Collaboration, Bailer-Jones et al. 2022).

on the construction of the *Gaia* DR3 source list can be found in Torra et al. (2021), while the basic inputs to the astrometric and G -band photometric processing (the G -band source image positions and fluxes) are described in Rowell et al. (2021). The validation of the astrometry and broad band photometry is summarised in Fabricius et al. (2021). The photometric pass-bands for G , G_{BP} , and G_{RP} are provided in Riello et al. (2021), and the one for G_{RVS} in Sartoretti et al. (2022b).

Finally, the *Gaia* Science Alerts project and content are described in Hodgkin et al. (2021).

3.1. G -band photometry for 6-p and 2-p sources

Section 7.2 of Gaia Collaboration, Brown et al. (2021) and Section 8.3 of Riello et al. (2021) describe a correction to be applied

to the G -band photometry for sources with 6-p and 2-p astrometric solutions. This correction was provided in the form of Python code and Astronomical Data Query Language (ADQL) recipes. *We note here that these corrections are included in Gaia DR3 and therefore should not be applied when working with photometry extracted from the Gaia DR3 data tables in the Gaia archive.*

As noted in Gaia Collaboration, Brown et al. (2021) the G -band photometry for a small number of sources is not listed in *Gaia* EDR3. This issue has not been fixed for *Gaia* DR3. The magnitudes can be found in a separate table to be provided through the *Gaia* DR3 ‘known issues’ web pages (for details see section 8.2 in Riello et al. 2021).

3.2. Celestial reference frame

Given that the astrometry in *Gaia* DR3 is unchanged from *Gaia* EDR3, it follows that the source positions and proper motions are provided with respect to the *Gaia*-CRF3, the third realisation of the Gaia celestial reference frame. *Gaia*-CRF3 is aligned with the third realisation of the International Celestial Reference Frame in the radio (ICRF3) to about 0.01 mas root-mean-square (RMS) at epoch J2016.0 (barycentric coordinate time, TCB), and globally non-rotating with respect to quasars to within $0.005 \text{ mas yr}^{-1}$ RMS. The *Gaia*-CRF3 is defined by the positions and proper motions of 1 614 173 QSO-like sources that were selected using *Gaia* EDR3 astrometry. For the alignment and spin of the *Gaia*-CRF3, the special sets of 2007 and 428 034 sources, respectively, were used based on the preliminary astrometric solutions known as AGIS3.1 (Lindgren et al. 2021b). The construction and properties of the *Gaia*-CRF3, the comparison to the ICRF3, and the procedure to fix the alignment and spin of the astrometric solution are described in Gaia Collaboration, Klioner et al. (2022).

3.3. Systematic errors

The systematic errors present in the astrometry and broad band photometry published in *Gaia* EDR3 carry over to *Gaia* DR3. The conclusions from investigations during the data processing for *Gaia* EDR3 astrometry were that the global parallax bias for *Gaia* DR3, as measured from quasars, is $-17 \mu\text{as}$. The RMS angular (i.e. source to source) covariances of the parallaxes and proper motions on small scales are $\sim 26 \mu\text{as}$ and $\sim 33 \mu\text{as yr}^{-1}$, respectively (see Lindgren et al. 2021b, for details). The parallax bias (and the proper motion systematic errors) varies as a function of magnitude, colour, and celestial position. This is extensively investigated in Lindgren et al. (2021a) and a recipe for correcting the parallaxes is given. The systematic errors in the broad band photometry are described in Riello et al. (2021).

Since the release of *Gaia* EDR3 several investigations of the systematic errors have been published. The parallax bias was investigated for specific sets of sources by Stassun & Torres (2021), and Ren et al. (2021) (eclipsing binaries); Huang et al. (2021) (Red Clump stars); Zinn (2021) (red giant branch stars with asteroseismic parallaxes); Wang et al. (2022) (red giant stars), Flynn et al. (2022) (stellar clusters); Groenewegen (2021), Kovacs & Karamicham (2021), Riess et al. (2021), and Molnar et al. (2022) (Cepheids and RR Lyrae stars); Maíz Apellániz (2022), and Maíz Apellániz et al. (2021) (Magellanic Clouds and globular clusters). The small-scale covariances are investigated in Zinn (2021), Vasiliev & Baumgardt (2021), and Maíz Apellániz et al. (2021), while assessments of the parallax uncertainties can be found in El-Badry et al. (2021), Vasiliev & Baumgardt (2021), and Maíz Apellániz et al. (2021).

The systematic errors in the proper motions and positions of stars in *Gaia* EDR3 were investigated by Cantat-Gaudin & Brandt (2021) and Lunz et al. (2021). Cantat-Gaudin & Brandt (2021) demonstrated that the proper motions of bright ($G \lesssim 13$) stars show a residual spin with respect to the fainter stars by up to $80 \mu\text{as yr}^{-1}$, and they provide a recipe to correct for this effect. Lunz et al. (2021) found differences in the alignment to the ICRF3 between bright and faint sources of about 0.5 mas. Systematic errors in the broad band photometry were investigated by Niu et al. (2021), Yang et al. (2021), and Thanjavur et al. (2021).

We stress here that including the above references does not imply an endorsement by the *Gaia* Collaboration of the results or any systematic error correction recipes provided in those papers.

Nevertheless, community efforts to investigate the quality of the *Gaia* data are highly appreciated and have in several cases led to an improvement in the validation procedures used during the *Gaia* data processing.

4. BP/RP spectra

BP/RP spectral observations are transmitted to the ground from the satellite in small windows surrounding the position of the source. The size of the BP/RP windows is 60 pixels AL by 12 pixels in the across scan (AC) direction, corresponding to an area in the sky of approximately $3.5''$ by $2.1''$. The size of the window affects the detection of sources in crowded regions, resulting in partially overlapping windows. These windows are excluded from the *Gaia* DR3 data processing. A special treatment will be implemented in future data releases.

4.1. Data processing

The BP/RP processing is described in detail in De Angeli et al. (2022) and Montegriffo et al. (2022). The spectra are first calibrated to an internal reference instrument which is homogeneous across all devices, observing configurations, and time. This is achieved purely from BP/RP data for a sufficiently large subset of sources selected to cover all calibration units (windowing strategies, gates, magnitude ranges, time). The internal calibration removes a number of effects such as bias, background, geometry, differential dispersion, and variations in response and in the line spread function (LSF) across the focal plane (Carrasco et al. 2021; De Angeli et al. 2022). The internal reference system is linked to the absolute system (both in terms of flux and wavelength) via the external calibration, which is based on a dedicated catalogue of spectro-photometric calibrators (Pancino et al. 2021a). More details concerning the calibration of the BP/RP spectral data to the absolute reference system are presented in Montegriffo et al. (2022).

We release mean low-resolution BP/RP spectra for about 220 million sources. They are selected to have a reasonable number of observations (more than 15 CCD transits) and to be sufficiently bright to ensure good signal-to-noise ratio (S/N), that is, $G < 17.65$. To this list, we add a few samples of specific objects that could be as faint as $G \sim 21.43$: about 500 sources used for the calibration of the BP/RP data, a catalogue of about 100 000 white dwarf candidates, 17 000 galaxies, about 100 000 QSOs, about 19 000 ultra-cool dwarfs, 900 objects that were considered to be representative for each of the 900 neurons of the self-organising maps (SOMs) used by the outlier analysis (OA) module (see section 9) and 19 solar analogues (De Angeli et al. 2022).

The S/N of the BP/RP spectra varies depending on the magnitude and colour of the source. In the range $9 < G < 12$, it can reach 1000 in the central part of the RP spectral range and it is of the order of 100 at $G \sim 15$. These spectra have been extensively used as input for further data processing inside DPAC (see e.g. sections 8, 9, 12), which provides a strong validation of their exceptional quality.

4.2. Data representation

The source mean spectra are provided in a continuous representation: they are described by an array of coefficients to be applied to a set of basis functions. We use a set of 55 basis functions for BP and 55 basis functions for RP (referred to as

‘bases’) defined as a linear combination of Hermite functions (Carrasco et al. 2021; De Angeli et al. 2022). In low-S/N spectra, as for instance at faint magnitudes, it is possible that higher order bases are over-fitting the noise in the observed data. In particular, low-S/N spectra when sampled in pseudo-wavelength can exhibit unrealistic features (wiggles). To mitigate this problem, Carrasco et al. (2021) suggest a statistical criterion to select the coefficients that can be dropped without losing information (truncation). Non-truncated and truncated spectra are in agreement within the noise. It should be noted that sharp features in the spectra, such as emission lines, can only be reproduced using higher order bases and therefore imply a larger number of significant coefficients. As the rejection criterion is statistical, it might happen that too few or too many coefficients are removed. This might affect faint objects with sharp spectral features, such as QSOs, or emission line stars. The effects of the truncation for various object classes are described in Sect. 3.4.3 of De Angeli et al. (2022).

To allow the users to decide how many coefficients are relevant for their scientific case, all the 55 coefficients of the basis functions are released. The number of coefficients returned by the truncation criterion is given in the parameters *bp_n_relevant_bases* and *rp_np_relevant_bases* available in the *xp_summary*³ table and in the mean continuous spectra available via Datalink⁴.

In addition to the continuous representation, sampled spectra representation (i.e. in the form of integrated flux vs. pixel) in both internal and absolute flux can be calculated using the Python package GaiaXPy made available with Gaia DR3 (see section 13). Sampling the spectra on a discrete grid in pseudo-wavelengths or absolute wavelengths results in a loss of information. In particular, the full covariance matrix is provided in the continuous representation, whereas it cannot be calculated in a spectrum sampled on a grid with more points than the number of basis function coefficients. Although sampled spectra are made available for a subset of sources in Gaia DR3, we strongly encourage users of the BP/RP spectra to make use of the continuous representation to maximise the scientific use of these data.

5. RVS data products

Gaia DR2 was the first release to include RVS radial velocities based on 22 months of data for stars at $G_{RVS} \leq 12$ and with effective temperatures $3500 < T_{\text{eff}} < 6900$ K.

Gaia DR3 contains newly determined radial velocities for about 33.8 million stars with $G_{RVS} \leq 14$ and with $3100 \leq T_{\text{eff}} \leq 14500$ K. Additional data products are published for the first time: v_{broad} for about 3.5 million stars, G_{RVS} magnitudes for more than 32 million stars, mean spectra for slightly less than 1 million stars, and epoch radial velocities for about 1000 RR Lyrae and roughly 800 Cepheids of different types (Ripepi et al. 2022). All these data come with quality parameters. Users are advised to treat the Gaia DR3 radial velocity catalogue as completely independent of Gaia DR2.

The spectroscopic pipeline and the improvements since Gaia DR2 are described in Chapter 6 of the online documen-

tation (Sartoretti et al. 2022a). All the products of the spectroscopic pipeline are available in the table *gaia_source*⁵, except for the mean spectra (see section 5.2). The transit radial velocities for the Cepheids and RR Lyrae stars are published in the table *vari_epoch_radial_velocity*⁶.

The products of the RVS pipeline, their properties, and their validation are described in more detail in dedicated papers: the radial velocity determination is described in Katz et al. (2022), the specific treatments to measure the hot star radial velocities in Blomme et al. (2022), and the radial velocity processing of the double-lined spectra is presented in Damerджи et al. (2022). The v_{broad} determination is discussed in Frémat et al. (2022) and the G_{RVS} magnitudes and the RVS pass-band in Sartoretti et al. (2022b).

For each valid RVS spectrum entering the pipeline, the transit radial velocity is computed through a fit of the RVS spectrum relative to an appropriate synthetic template spectrum. In Gaia DR3, for stars cooler than 7000 K, the template input parameters are mostly taken from intermediate results of Apsis (Creevey et al. 2022) based on Gaia DR2 BP/RP spectra (see section 9). For hotter stars, they were derived as explained in Blomme et al. (2022).

5.1. Data processing improvements

A number of improvements were implemented in the Gaia DR3 RVS pipeline. Here we list the most significant. Bright stars are processed using the method already implemented in Gaia DR2, that is, the combined radial velocity for stars at $G_{RVS} < 12$ is the median of the single-transit radial velocities. However, this method is not very efficient when the S/N is low. The radial velocities of faint stars in the range $12 < G_{RVS} < 14$ mag are obtained from the averaged single-transit cross-correlation functions referring to the Solar System barycentre.

To improve performance at the faint end, we implemented an improved stray-light-correction procedure. The correction map is estimated every 30 hours from the faint-star spectra edges and from the virtual objects⁷, while in Gaia DR2 a single stray-light map was computed from the Ecliptic Pole scanning law⁸ data.

We introduce a deblending procedure when the transit spectra are contaminated by nearby sources falling inside the RVS window. These deblended spectra are then used to obtain radial velocities and mean spectra, while in Gaia DR2 they were simply removed from the pipeline. This allows us to process a larger number of epoch spectra per source, increasing the S/N. However, we point out that only the clean non-blended transits are used to derive G_{RVS} , and v_{broad} .

The LSF was calibrated in both the AL and AC directions. The LSF-AL calibration has reduced the systematic shifts between the two fields of view affecting the wavelength calibration zero point and the epoch radial velocities. The LSF-AC calibration was also used in the deblending procedure and in the es-

⁵ https://gea.esac.esa.int/archive/documentation/GDR3/Gaia_archive/chap_datamodel/sec_dm_main_source_catalogue/sssec_dm_gaia_source.html

⁶ https://gea.esac.esa.int/archive/documentation/GDR3/Gaia_archive/chap_datamodel/sec_dm_variability_tables/sssec_dm_vari_epoch_radial_velocity.html

⁷ Virtual objects are empty windows acquired on a predefined pattern for calibration purposes

⁸ During the early weeks of the mission, the Gaia spin axis followed the Sun on the ecliptic, scanning the North and South Ecliptic Poles every six hours (see Gaia Collaboration, Prusti et al. 2016, Section 5.2)

³ https://gea.esac.esa.int/archive/documentation/GDR3/Gaia_archive/chap_datamodel/sec_dm_spectroscopic_tables/sssec_dm_xp_summary.html

⁴ Datalink is an IVOA protocol that specifies a service container which can represent or accommodate a variety of services. Tutorials on the access to Gaia Datalink products can be found at <https://www.cosmos.esa.int/web/gaia-users/archive/ancillary-data>

timation of the flux lost outside the window for estimation of G_{RVS} .

v_{broad} is computed for each transit, excluding deblended spectra, and then averaged. In addition to the projected rotational velocity, $v \sin i$, v_{broad} can include other physical effects like macro-turbulence, residual instrumental effects (LSF model uncertainty), and template mismatches.

We consider that a spectrum can be contaminated by nearby sources with $G_{RVS} < 15$ even if they are not located inside the RVS window. In that case, the target spectrum is removed when the contaminant differs from the target source by less than 3 mag. This effect was neglected in *Gaia* DR2.

Finally, G_{RVS} ($grvs_mag$ in *gaia_source*) is calculated as the median of the single-transit G_{RVS} measurements. Values of G_{RVS} fainter than 14.1 were regarded as spurious and removed because they could have been caused by an inaccurate background estimate.

5.2. RVS spectra

The published mean RVS spectra are identified using the column *has_rvs* in the *gaia_source* table. Their spectra are available through the Datalink interface in the table *rvs_mean_spectrum*⁹. The mean spectra and their processing are described in detail in Seabroke et al. (2022). In summary, the transit RVS spectra are extracted, cleaned, deblended (if needed), wavelength calibrated and normalised either to their pseudo-continuum or by scaling with a constant (the latter for cool stars or noisy spectra). The spectra are then shifted to the rest frame using the epoch radial velocities for the bright stars for $G_{RVS} \leq 12$ mag, or using the combined radial velocity for the faint stars; they are then interpolated into a common wavelength array spanning 846–870 nm with a step of 0.01 nm and averaged. S/N information is also provided in the table *gaia_source*.

The released RVS spectra are selected from among stars of spectral type AFGK with S/N > 20. In addition, a sample of low-S/N spectra spanning all spectral types is added (see Seabroke et al. 2022). A known issue is that the published spectra are not uniformly distributed over the sky.

5.3. Caveats

The contamination of the flux of an RVS target source by the flux of a nearby bright source can produce a spurious population of stars with high radial velocities. This issue was known from *Gaia* DR2 (Seabroke et al. 2021). In addition bright-star contamination produces biased radial velocities which do not necessarily stand out from the overall radial velocity distribution when two sources are separated by 1.8'' in the direction perpendicular to the scan. These stars were removed from the catalogue (Katz et al. 2022).

Radial velocity uncertainties are generally very small, of the order of a few km s^{-1} or even less than 1 km s^{-1} at the bright end. However, they are slightly underestimated for bright stars. A correction is proposed in Babusiaux et al. (2022).

6. Variables

The approach to the variability analysis in successive data releases is iterative, including at each data release more variability

types with lower signal to noise. In *Gaia* DR3 we publish a total of more than 10 million variable sources in about 24 variability types (and their time series), in addition to approximately 2.5 million galaxies. The two-dimensional structure of galaxies is observed by *Gaia* over a range of position angles. This can induce spurious (non-intrinsic) photometric variability. This effect is used to identify galaxies, but their time series are not released.

The *Gaia* DR3 variability content is a great leap in comparison with *Gaia* DR2 where we reached more than 550 000 stars, with six variability types.

In the variability pipeline (VARI) processing, the variability was first tested in the time domain, and was then characterised in the Fourier domain and classified by multiple classifiers. We refer to the documentation and to Eyer et al. (2022, and references therein) for more processing details. The input data are mostly the time series of field-of-view transits of the broad band photometry in the calibrated G , G_{BP} , and G_{RP} bands. Additionally, for Cepheid and RR Lyrae stars we use radial velocity time series from the RVS instrument (see section 5.2) (Ripepi et al. 2022; Clementini et al. 2022); the long-period variable (LPV) analysis included RP spectral time series (which are not part of *Gaia* DR3, Lebzelter et al. 2022); and short-timescale variables are based on per-CCD G -band photometry. We refer to Distefano et al. (2022) for more information about solar-like variables; Marton et al. (2022) for young stellar objects; Wyrzykowski et al. (2022) concerning microlensing events; Gomel et al. (2022) for ellipsoidal variables with possible compact object secondaries; and Carnerero et al. (2022) for information on active galactic nuclei (AGN) candidates. Candidate eclipsing binaries are described in Mowlavi et al. (2022). A subset of those also have parameters in the NSS tables (see section 7).

Variability products in *Gaia* DR3 can be accessed as follows. In the *gaia_source* table the field *phot_variable_flag* is set to 'VARIABLE' when a source appears in any of the *vari_** tables, except for the *vari_summary*¹⁰ table which includes non-variable sources that appear in GAPS (see below). The *vari_summary* table lists statistical parameters for all variable sources and all sources in GAPS. The time series in G , G_{BP} , and G_{RP} bands of all sources listed in the *vari_summary* table are available as light curve data through the Datalink interface.

The quality of this data base is impressive. For instance, concerning LPVs, the catalogue includes about 1.7 million sources with G variability amplitudes greater than 0.1 mag (0.2 mag in *Gaia* DR2). The period is derived for about 392 000 of them. In *Gaia* DR2 we only identified about 151 000 LPV sources. Concerning *Gaia* DR3 data, in many cases it was possible to identify the spectral class from RP spectra, that is, cool giants of spectral types M (oxygen-rich) and C (carbon-rich). This classification was based on the presence in the RP spectra of numerous molecular absorption bands, mainly those due to TiO and related oxides for M-type and molecular bands mostly associated with CH and C₂ molecules for C-type stars (Lebzelter et al. 2022).

More than 270 000 confirmed RR Lyrae stars are released in *Gaia* DR3, almost doubling the *Gaia* DR2 RR Lyrae catalogue. In addition, we provide a better characterisation of the RR Lyrae pulsational and astrophysical parameters. This, along with the improved astrometry published with *Gaia* EDR3, make this sample the largest, most homogeneous all-sky catalogue of RR Lyrae stars published so far (Clementini et al. 2022).

⁹ https://gea.esac.esa.int/archive/documentation/GDR3/Gaia_archive/chap_datamodel/sec_dm_spectroscopic_tables/ssec_dm_rvs_mean_spectrum.html

¹⁰ https://gea.esac.esa.int/archive/documentation/GDR3/Gaia_archive/chap_datamodel/sec_dm_variability_tables/ssec_dm_vari_summary.html

A small, but significant number of micro-lensing event candidates (363 in total, of which 90 are new) are identified (Wyrzykowski et al. 2022). While testing the exoplanet detection method, two *Gaia*-discovered transiting extra-solar planets were found from the epoch photometry (Panahi et al. 2022). This demonstrates the feasibility of the detection approach and *Gaia*'s potential for discovering exoplanet candidates. About 214 exoplanet candidates are released in *Gaia* DR3.

A large number of ellipsoidal variable candidates were detected. Their variability is due to the tidal interaction with a companion in a close binary system. About 6000 short-period ellipsoidal variables have relatively large-amplitude modulations in G , possibly indicating a massive, unseen secondary. Among those, 262 systems have a higher probability of having a compact secondary. Follow-up observations are needed to verify the true nature of these variables (Gomel et al. 2022).

6.1. *Gaia* Andromeda Photometric Survey

The photometric time series for all *Gaia* sources located within a 5.5° radius centred on the Andromeda galaxy are part of GAPS, which contains more than 1.2 million sources. Whether or not a source appears in the GAPS survey is indicated in the *gaia_source* table by setting the field *in_andromeda_survey* to 'true'. The time-series statistics for GAPS sources are available in the *vari_summary* table. Evans et al. (2022) give more details.

6.2. Caveats

As a caveat, a number of sources show more than one type of variability. In general this overlap can be scientifically explained. However, this is not always the case, for instance a few objects were classified as both long period and short timescale (Lebzelter et al. 2022). Holl et al. (2022) discuss spurious periodic variations in the photometric data, due to instrumental effects.

7. Non-single stars

About 800 000 solutions for NSS including astrometric (Halbwachs et al. 2022), spectroscopic (single lined SB1; and double lined SB2) (Gosset et al. 2022), and eclipsing binaries (Siopis et al. 2022) are published in *Gaia* DR3, with either orbital elements or trend parameters, or combinations of these.

7.1. NSS archive tables

The NSS tables are organised according to the type of solution: *nss_two_body_orbit*¹¹ contains the orbital parameters for all the binary categories; *nss_acceleration_astro*¹² contains accelerations for sources with an astrometric motion better described using a quadratic or cubic proper motion; *nss_non_linear_spectro*¹³ presents trend (long period) solutions

¹¹ https://gea.esac.esa.int/archive/documentation/GDR3/Gaia_archive/chap_datamodel/sec_dm_non--single_stars_tables/ssec_dm_nss_two_body_orbit.html

¹² https://gea.esac.esa.int/archive/documentation/GDR3/Gaia_archive/chap_datamodel/sec_dm_non--single_stars_tables/ssec_dm_nss_acceleration_astro.html

¹³ https://gea.esac.esa.int/archive/documentation/GDR3/Gaia_archive/chap_datamodel/sec_dm_non--single_stars_tables/ssec_dm_nss_non_linear_spectro.html

of spectroscopic binaries; *nss_vim_fl*¹⁴ includes objects that exhibit photocentre displacements due to the photometric variability of one component, requiring the correction of the astrometric parameters.

This catalogue outnumbers existing surveys by large factors, spanning a large range of binary types, periods, and magnitudes. The potential of the *Gaia* DR3 binary star content is outlined in [Gaia Collaboration, Arenou et al. \(2022\)](#).

7.2. Caveats

Binaries can simultaneously belong to different classes; for example, astrometric binaries can also be spectroscopic binaries (identified as *astroSpectroSB1* in the *nss_solution_type* in the table *nss_two_body_orbit*) or eclipsing binaries can also be spectroscopic binaries (identified as *eclipsingSpectroSB1*). In many cases of multiple solutions, combined solutions have been computed and included in the *Gaia* DR3 catalogue. However, combined solutions are not always provided, and sources can be found in several tables simultaneously. More information and advice on how to deal with these cases can be found in [Gaia Collaboration, Arenou et al. \(2022\)](#).

Acceleration solutions are not always in agreement with expectations from known orbits in external catalogues, and a fraction of them could have had an orbital solution. In general the parallaxes and proper motions derived by the NSS processing are more precise than those derived by the *Gaia* astrometric global iterative solution (see section 3) which assumes that all stars are single. This is not always the case for the acceleration solutions, which should be used with caution ([Gaia Collaboration, Arenou et al. 2022](#); [Babusiaux et al. 2022](#)).

Spurious solutions around the satellite precession period (62.97 days) or for some short periods can be found for SB1. Formal uncertainties are not rescaled according to the goodness of fit for all the binary types, but only for the astrometric solutions. The NSS sample is far from complete. This is because of a number of selection effects due to data processing and additional filtering. Statistical studies on the data should take this into account.

8. Solar System objects

In *Gaia* DR3, about 160 000 SSOs were processed and analysed. As in previous data releases, known SSOs are searched for by matching the observed transits to computed transits based on the information on the satellite orbit, the scanning law, and a numerical integration of the SSO motion. Tanga et al. (2022) gives a description of the selection and processing. After filtering the list for possible contaminants, the final input selection had 3 513 248 transits for 156 837 known asteroids. Planetary satellites were also added following a similar procedure. In total, 31 planetary satellites are included. In addition, *Gaia* DR3 includes the astrometry of unknown moving sources based on the AL motion of objects observed from December 2016 to June 2017. The final input list of unidentified SSOs for *Gaia* DR3 comprises 4522 transits, corresponding to 1531 groups of chained transits of objects that at the time of processing were considered unmatched. Later, Tanga et al. (2022) identify 712 SSOs. These sources still

¹⁴ https://gea.esac.esa.int/archive/documentation/GDR3/Gaia_archive/chap_datamodel/sec_dm_non--single_stars_tables/ssec_dm_nss_vim_fl.html

appear as unmatched in the table *sso_source*¹⁵. It cannot be excluded that some of the still unmatched sources can be linked to known objects.

The astrometric accuracy of the orbits is impressive and remains at sub-mas level for $G < 17$, reaching an exceptional value of ~ 0.25 mas for $12 < G < 15$ mag.

Gaia DR3 contains spectro-photometry for more than 60 000 asteroids the majority of which have been observed with G between ~ 18 and 20. The internally calibrated BP/RP epoch spectra are divided by the solar analogue spectrum to obtain epoch reflectance spectra that are subsequently averaged and sampled in 16 bands in wavelength. Only spectra derived using more than three epochs and with an average S/N of higher than 13 are published. No further rejection is applied. Poor spectra are flagged on a wavelength-by-wavelength basis introducing the *sso_reflectance_spectrum_flag*¹⁶, an array of 16 integers, one for each wavelength of the spectral bands (Gaia Collaboration, Galuccio et al. 2022). The main properties of the reflectance spectra are described in section 12.

9. Object characterisation

Gaia DR3 includes APs for stars, galaxies, and QSOs. About 1600 million objects have class probabilities ($G < 21$), about 470 million stars have stellar parameters ($G < 19$), and there are about 6 million QSOs and about 1.3 million galaxy candidate redshifts. More details can be found in Creevey et al. (2022) concerning the AP content and an overview of the methods used in the software (Apsis) to produce these data.

9.1. Data processing

In total, 13 modules in the Apsis software provide 43 primary APs along with auxiliary parameters in 538 fields which appear in ten tables of the *Gaia* archive. A subset of APs is available in *gaia_source*. The astrophysical characterisation makes use of *Gaia* EDR3 broad band photometry and parallaxes, and *Gaia* DR3 mean RVS spectra and internally calibrated sampled mean BP/RP spectra. The stellar APs comprise atmospheric properties, evolutionary parameters, metallicity, individual chemical element abundances, and extinction parameters, along with other characterisation such as equivalent widths of the $H\alpha$ line and activity index for cool active stars.

The discrete source classifier (DSC) produces the object classification, that is, it assigns class probabilities to all sources for five main classes, using different classifiers; these classes are QSO, galaxy, star, white dwarf, and physical binary star. The result of this classification is then used by four modules to initiate the processing of galaxies, QSOs, outliers, and extinction. The unresolved galaxy classifier (UGC) and the QSO classifier (QSOC) modules (Delchambre et al. 2022) provide redshifts for candidate galaxies and QSOs. A more detailed discussion about the *Gaia* DR3 extragalactic content can be found in section 11.

The OA module performs an unsupervised classification for sources with lower probabilities from DSC, using SOMs (Kohonen 2001). OA groups similar objects into neurons on a 30×30

grid according to the similarity of their BP/RP spectra, as reported in *oa_neuron_information*¹⁷ (see Creevey et al. 2022, figure 11, for examples). Other multi-dimensional data comprise a total Galactic extinction map at four healpix levels as well an optimal-level map derived by the total Galactic extinction module (TGE). The above data products are detailed in Delchambre et al. (2022).

For the stellar and interstellar medium characterisation, the General Stellar Parametriser for Photometry (GSP-Phot) derives astrophysical parameters (T_{eff} , $\log g$, A_G , distance, ...) from BP/RP spectra down to $G = 19$ assuming they are all stars (Andrae et al. 2022). The multiple source classifier (MSC) derives similar stellar parameters under the hypothesis that all objects are unresolved binaries using the same input data as GSP-Phot. The General Stellar Parametriser for Spectroscopy (GSP-Spec) derives atmospheric parameters using the mean RVS spectra. It additionally derives 13 chemical species and diffuse interstellar band (DIB) equivalent widths (see Recio-Blanco et al. 2022, for details). Other modules analyse only a selected class of objects. This is the case for the Extended Stellar Parametrisers (ESPs) dealing with emission line stars (ESP-ELS), hot stars ($7000 < T_{\text{eff}} < 50\,000$ K, ESP-HS), cool stars (ESP-CS), and ultra-cool dwarfs ($T_{\text{eff}} < 2500$ K, ESP-UCD). These modules together produce T_{eff} and $\log g$ but also $v \sin i$, spectral type classifications, $H\alpha$ equivalent widths, and chromospheric activity index (using the calcium infrared triplet in the RVS domain (Lanzafame et al. 2022)).

The Final Luminosity Age Mass Estimator (FLAME) derives evolutionary parameters from data that are processed by GSP-Phot and GSP-Spec. These comprise the stellar radius, luminosity, gravitational redshift, mass, age and evolutionary stage for stars. All of these data products appear in the *astrophysical_parameters*¹⁸ and *astrophysical_parameters_supp*¹⁹ tables in the *Gaia* archive. In addition to these data products, Markov Chain Monte Carlo (MCMC) samples are provided for two of the modules, GSP-Phot and MSC through the Datalink interface.

To date, this is the most extensive catalogue of astrophysical parameters homogeneously derived. It is based on *Gaia*-only data, and it will be superseded only by the fourth data release, *Gaia* DR4. Until then, it will remain the reference for upcoming ground- and space-based surveys. References to some applications and advice on the use of the APs can be found in the papers listed in section 12.

9.2. Caveats

The AP quality, although quite reliable on average, does vary depending on the quality of the input data (parallaxes, magnitudes, and spectra) but it can also vary based on the assumptions in the methods. The users should be aware of several issues. Variability is not taken into account in the processing, because only mean spectra and mean broad band magnitudes are used as input. Therefore, parameters of stars showing large variability might be inaccurate.

¹⁵ https://gea.esac.esa.int/archive/documentation/GDR3/Gaia_archive/chap_datamodel/sec_dm_solar_system_object_tables/ssec_dm_sso_source.html

¹⁶ https://gea.esac.esa.int/archive/documentation/GDR3/Gaia_archive/chap_datamodel/sec_dm_solar_system_object_tables/ssec_dm_sso_reflectance_spectrum.html

¹⁷ https://gea.esac.esa.int/archive/documentation/GDR3/Gaia_archive/chap_datamodel/sec_dm_astrophysical_parameter_tables/ssec_dm_oa_neuron_information.html

¹⁸ https://gea.esac.esa.int/archive/documentation/GDR3/Gaia_archive/chap_datamodel/sec_dm_astrophysical_parameter_tables/ssec_dm_astrophysical_parameters.html

¹⁹ https://gea.esac.esa.int/archive/documentation/GDR3/Gaia_archive/chap_datamodel/sec_dm_astrophysical_parameter_tables/ssec_dm_astrophysical_parameters_supp.html

APs derived for objects in high-density regions are affected by crowding. For instance $[M/H]$ in the core of a dense cluster can significantly differ from the value in the outskirts.

GSP-Phot distance estimates are underestimated for sources with large parallax errors because of an extinction prior which then dominates the distance inference. GSP-Phot metallicity is poorly derived for metal-poor stars ($[M/H] < -1$), and a metallicity calibration tool is proposed to the users to calibrate these. The data show residual degeneracy among the parameters, for instance T_{eff} and the extinction in the G , A_G , from GSP-Phot.

MSC treats all stars as unresolved binaries in BP/RP spectra; DSC shows poor performance on the classification of physical binaries and white dwarfs.

Additional information about the limitations of the APs are detailed in Babusiaux et al. (2022), while both the quality and validation of the stellar and non-stellar content are discussed more extensively in Fouesneau et al. (2022) and Delchambre et al. (2022), respectively. In general, users are advised to use quality flags and follow the recommendations detailed in the above papers.

10. Extended objects

The *Gaia* on-board system is designed to detect point-like sources (de Bruijne et al. 2015). However, EOs such as galaxies and galaxies hosting a QSO can be detected if their central region is sufficiently compact and bright. In this case, it is possible to reconstruct a two-dimensional light profile of the extended source. At each passage *Gaia* observes the nine one-dimensional Astro Field (AF) windows and the two-dimensional Sky Mapper (SM) windows. As the scan angle changes from one observation to the next, after a sufficient number of transits a large part of the source is covered by the observations. Dedicated software can combine the observed windows on ground to infer the two-dimensional light profile parameters. During the first 34 months of operations about 116 million transits in the AF and SM focal planes were collected and processed. The EO pipeline compares the observations with a large number of simulations of galaxy images deriving the best-fit surface brightness profile parameters.

The lists of objects that were processed are derived from external catalogues. The list of QSOs was set up by merging the major catalogues of QSOs or AGN candidates published before 2018. In addition, we make use of an unpublished selection of candidates based on *Gaia* DR2 QSOs, and classified on the basis of their photometric variability (Rimoldini et al. 2019). The list of galaxies was derived from a preliminary analysis of *Gaia* DR2 sources with a match in the allWISE catalogue (Cutri et al. 2013). An unsupervised heuristic method (Krone-Martins et al. 2022) selects sources for a subsequent analysis. More than 1 million previously identified QSOs are analysed, identifying a host galaxy around approximately 64 000 of them. The surface brightness profiles of the host is published for a subset of about 15 000 QSOs, with a robust solution. Their Sérsic indexes indicate that they are mostly disc-like galaxies. Concerning the galaxy sample, two profiles are published (a free Sérsic profile and a de Vaucouleurs one). About 940 000 galaxies were analysed and robust solutions were derived for about 914 000 of them. The distribution of the parameters indicates that *Gaia* mostly detects elliptical galaxies.

These data can be found in the *Gaia* DR3 tables *qso_candidates*²⁰ and *galaxy_candidates*²¹. Details on the data processing and input lists can be found in Ducourant et al. (2022). This impressive data base is the first all-sky catalogue of two-dimensional light-profile parameters of galaxies, and QSO host galaxies derived at a resolution of about 200 mas.

The use of input lists clearly favours purity over completeness, even if a residual contamination by stars is still present.

Gaia observations are limited to the central area of the galaxy. For this reason, the derived brightness profile parameters do not always agree with external catalogues (Babusiaux et al. 2022; Ducourant et al. 2022).

11. *Gaia* DR3 extragalactic content

Extragalactic objects are classified or analysed by several modules in the *Gaia* data-processing system using various input data and methods. An overview of the extragalactic processing and content in *Gaia* DR3 is given in *Gaia* Collaboration, Bailer-Jones et al. (2022).

A predefined list of objects is analysed to derive the surface brightness profiles by the EO module. Classification of extragalactic objects is performed independently by two modules: the VARI module uses photometric light curves, whereas DSC uses the BP/RP spectra and astrometry. The modules QSOC and UGC estimate the redshifts of QSO and galaxy candidates (respectively) identified by DSC. Finally, the OA module performs a clustering of low-probability classifications from DSC.

The fact that different methods, input data, and training data are used to classify or select extragalactic objects has an important consequence: there is no common definition of QSOs or galaxies across the various *Gaia* modules. DSC and OA focus on completeness rather than purity. UGC processes objects with a higher probability of being galaxies according to the DSC classification, whereas QSOC uses a very low threshold on the DSC QSO probability, in order to analyse as many sources as possible. As a result, the sample of QSO candidates with redshifts is complete rather than pure, whereas that of the galaxy candidates with redshifts is of higher purity, although some contamination remains (see below).

11.1. Extragalactic object tables

Each one of the above modules provides independent results that are available across several tables. The table *astrophysical_parameters* lists all the parameters produced by DSC. The *oa_neuron_information* contains the SOMs from the OA module. The tables *vari_classifier_result*²² and *vari_agn*²³ present the parameters of the AGNs identified through the photometric light-curve analysis. From the above tables, we produce two integrated tables in *Gaia* DR3, *qso_candidates* and *galaxy_candidates*, where all good QSO and galaxy candidates

²⁰ https://gea.esac.esa.int/archive/documentation/GDR3/Gaia_archive/chap_datamodel/sec_dm_extra--galactic_tables/ssec_dm_qso_candidates.html

²¹ https://gea.esac.esa.int/archive/documentation/GDR3/Gaia_archive/chap_datamodel/sec_dm_extra--galactic_tables/ssec_dm_galaxy_candidates.html

²² https://gea.esac.esa.int/archive/documentation/GDR3/Gaia_archive/chap_datamodel/sec_dm_variability_tables/ssec_dm_vari_classifier_result.html

²³ https://gea.esac.esa.int/archive/documentation/GDR3/Gaia_archive/chap_datamodel/sec_dm_variability_tables/ssec_dm_vari_agn.html

are listed. The selection rules are detailed in [Gaia Collaboration, Bailer-Jones et al. \(2022\)](#). The *gaia_source* table includes the DSC classification probability as well as two flags, *in_qso_candidates* and *in_galaxy_candidates*, which indicate the presence of the source in the integrated table(s).

Already in *Gaia* EDR3, a list of 1.6 million compact extragalactic sources was used to define the *Gaia*-CRF3 ([Gaia Collaboration, Klioner et al. 2022](#)). These sources were identified from *Gaia* EDR3 astrometry by means of positional cross-matching with 17 external catalogues of QSOs and AGNs, and were subsequently filtered using astrometric criteria to remove stellar contaminants. The sample spans a magnitude range $13.4 < G < 21.4$ with a median positional error of 0.45 mas. By construction this sample is of high purity.

11.2. Completeness and purity

The integrated tables of extragalactic objects favour completeness over purity. *qso_candidates* contains 6.6 million candidate QSOs and *galaxy_candidates* contains 4.8 million candidate galaxies, with global purities estimated to be 50% and 70% respectively. Contamination is mostly due to the fact that there are many more stars in the *Gaia* survey, and arises in part from the choice of probability classification threshold for inclusion. Furthermore, some modules chose not to filter out regions such as the Magellanic Clouds and the Galactic plane, which are dense regions of stars and therefore also of contaminants. A very small fraction of sources are too bright to be genuine QSOs or galaxies. The same astrometric filtering as for *Gaia*-CRF3 applied to the content of the integrated QSO table *qso_candidates* gives a set of ~ 1.9 million sources, which are identified by the flag *astrometric_selection* ([Gaia Collaboration, Bailer-Jones et al. 2022](#)). Purer subsets of the two tables, containing ~ 1.9 million probable QSOs and ~ 2.9 million probable galaxies (both with around 95% purity) can be selected using the queries on EO, DSC, and VARI quality flag parameters listed in [Gaia Collaboration, Bailer-Jones et al. \(2022\)](#). Concerning QSOs, this new sample has about 1.8 million sources in common with the astrometric sample.

Finally, the DSC star class could be used to select a purer star sample, rejecting objects that are in the *qso_candidates* or *galaxy_candidates*, that is, those identified as candidate galaxies, QSOs, or extended objects. However, concerning extended objects, the DSC has not used morphological information in its classification (see for details [Delchambre et al. 2022](#)). Indeed there is no general morphological classification in *Gaia* DR3. Only a limited number of galaxy and QSO candidates (based on non-*Gaia* data) were analysed for evidence of a host galaxy using 2D morphology built up from the 1D scans (see section 10). As a consequence, residual contamination from extragalactic sources can still be present in a star sample selected following the above criteria.

12. The scientific performances of the catalogue

The scientific quality and the potential of the *Gaia* DR3 data are demonstrated in a number of accompanying papers providing basic science applications and additional validation of the catalogue. These illustrate the limitations of the data, providing advice and guidance to the users on specific scientific problems. The following topics are treated.

[Gaia Collaboration, Creevey et al. \(2022\)](#) present clean samples of very high-quality astrophysical parameters of stars derived from low-resolution BP/RP and RVS spectra all across the

HR diagram, selected through severe quality cuts. These data have a long-term legacy value for future follow-up studies and missions and are released together with *Gaia* DR3 in separate tables. These samples include about 3 million OBA young disc stars, roughly 3 million FGKM stars, and about 21 000 ultra-cool dwarfs. [Gaia Collaboration, Creevey et al. \(2022\)](#) identify specific subsamples of particular interest to the community such as approximately 6 000 solar-analogues and 15 000 carbon stars, and provide homogeneous parameters for a subsample of the 111 *Gaia* spectro-photometric standard stars defined by [Pancino et al. \(2021b\)](#). For the ultra-cool dwarfs *Gaia* and 2MASS data are combined to provide radius and luminosity.

[Gaia Collaboration, Recio-Blanco et al. \(2022\)](#) use *Gaia* astrometry, radial velocities, chemo-dynamical analysis of disc and halo populations, producing the largest all-sky chemical map to date and analysing the abundances of streams from accretion events. This map includes chemical information for 597 open clusters, which represents the largest compilation of abundances homogeneously derived for clusters.

[Gaia Collaboration, Schultheis et al. \(2022\)](#) discuss the distribution of the DIB at 862 nm in the RVS spectral range in connection with the interstellar extinction to within a few kiloparsecs of the Sun. The paper provides the most precise measurement to date of the rest frame wavelength of the DIB at 8620.86 ± 0.019 Å.

[Gaia Collaboration, Drimmel et al. \(2022\)](#) explore non-axisymmetric features in the disc of the Milky Way in both configuration and velocity space. These authors use *Gaia* DR3 APs and variability classifications to select various stellar populations in the disc of the Milky Way, tracing the spiral structure up to 4–5 kpc from the Sun. About 6 million red giant branch stars allow the authors to map the velocity field in the disc up to 8 kpc from the Sun, allowing the detection of signatures of the Galactic bar.

[Gaia Collaboration, Arenou et al. \(2022\)](#) present a clean catalogue of binary stars, discussing its completeness and some statistical features of the orbital elements in comparison with external catalogues. In addition, a catalogue of tens of thousands of stellar masses is provided. Several compact object candidates are identified. The catalogue includes sources found in rare evolutionary stages such as EL CVn, underlining the potential of analysing both photometric and orbital data. New binary UCD candidates are discovered and their masses estimated; two new exo-planets are found, and several dozen candidates are identified. The catalogue is made available together with *Gaia* DR3 tables.

[Gaia Collaboration, Galluccio et al. \(2022\)](#) present reflectance spectra, derived from BP/RP spectra, for SSOs, discussing their statistical properties. The $(z - i)$ colours are derived from the spectra, where z and i represent the values of the reflectances estimated with spline interpolation at 748 and 893 nm, respectively. $(z - i)$ allows the identification of asteroid families sharing similar properties and common origin. An interesting feature is that the spectral slope²⁴ of the mean reflectance spectra and the depth of the 1 μ m absorption band seem to show an increase with time for the S-type family, which is possibly due to space weathering effects on the asteroid surfaces. The catalogue is included in the data release.

[Gaia Collaboration, Montegriffo et al. \(2022\)](#) demonstrate the potential of synthetic photometry obtained from flux-calibrated BP/RP spectra for pass-bands fully enclosed in the

²⁴ the spectral slope is derived by fitting the mean reflectance spectra in the wavelength range 450 and 760 nm with a straight line and taking the angular coefficient

Gaia wavelength range. This photometry has been used internally for validation purposes. Synthetic photometry in various photometric systems can be produced using the Python package *GaiaXPy* (see section 13). High-quality external photometry in large and medium passbands is reproduced at a few percent level in general and up to the milli-mag level when the synthetic photometry is standardised using an external reference catalogue. For a subset of 13 wide and medium bands, we release the *Gaia* Synthetic Photometry Catalogue (GSPC), an all-sky space-based catalogue of standardised photometry for the majority of the stars with released spectra and $G < 17.65$. A separate catalogue contains synthetic photometry in a selection of relevant bands for 100 000 white dwarfs selected from *Gaia* EDR3.

Lastly, *Gaia* Collaboration, De Ridder et al. (2022) investigate the properties of high-mass main sequence pulsators, showing that *Gaia* DR3 data are precise and accurate enough to identify nearby OBAF-type pulsators.

13. Software tools

A number of Python software tools²⁵ are made available to the scientific community. The following are some examples.

- The Python package *GaiaXPy* which offers the possibility to compute synthetic photometry from BP/RP spectra in various photometric systems (see *Gaia* Collaboration, Montegriffo et al. 2022, and Sect. 12), and to simulate BP/RP mean spectra from a custom input absolute spectral energy distribution. In addition sampled mean spectra can be derived from the continuous basis function representation. Detailed information can be found in *De Angeli et al. (2022)*.
- A tool to re-calibrate the GSP-Phot metallicity output (see *Creevey et al. 2022*, Appendix E for detail) based on comparison with external surveys.
- A package to re-calibrate the GSP-Spec metallicity, $[\alpha/\text{Fe}]$, and $\log g$ (*Recio-Blanco et al. 2022*).
- A script to derive bolometric corrections for the stars analysed by FLAME.
- A package to extract the extinction as a function of Galactic coordinates from the two-dimensional TGE Galactic maps.
- A tool to visualise the neurons in the OA SOMs.
- A tutorial on the programmatic download of large sets of Datalink items (> 5000 elements).
- Examples of cone search scripts.

We point out that the GSP-Phot and GSP-Spec re-calibration tools proposed here have their own limitations, as described in the related documentation. They provide tentative expressions to be used at the discretion of the user, depending on the science case.

14. Conclusions

Gaia DR3 expands *Gaia* EDR3 with a rich and large set of data products containing detailed astrophysical information for the same source catalogue. The quantity, quality and variety of astrophysical data constitute a major advance in the series of *Gaia* data releases. This release includes the largest collection of all-sky spectrophotometry and radial velocities and the largest collection of variable sources ever produced. The availability of

APs from low- and high-resolution spectra greatly surpasses existing catalogues. This catalogue includes a spectrophotometric and dynamical survey of SSOs of the highest accuracy. The NSS content outnumbers all existing binary star catalogues, and *Gaia* DR3 also contains the first all-sky space-based survey of QSO host and galaxy two-dimensional light profiles.

In this paper we briefly summarise the main additions and improvements to the data processing and we include comments on the data quality. However, the *Gaia* DR3 data products are numerous and complex and not all the details could be presented here. A more complete overview, insights into known issues with the data, and advice on the use of the data can be found in the papers accompanying the release and in the online documentation.

The nominal *Gaia* mission ended on July 2019. The mission has been extended since then to the end of 2022, with an indicative approval to extend the mission to the end of 2025. In 2025, the propellant for the micro-propulsion system is expected to be exhausted, and the precision on the attitude and spin rate of the satellite required for the astrometry can then no longer be maintained. At this point, the *Gaia* mission end of life will be reached and over 10 years of data will have been collected. In this context, two further data releases are foreseen, *Gaia* DR4 and *Gaia* DR5 which will include the data from the extended mission. *Gaia* DR4 will be based on 66 months of data, including a six-month period when the satellite was operated with a reversed direction of the precession of the spin axis around the direction to the Sun. This will mitigate the degeneracy between the across scan motion of the sources and their parallaxes, reducing this specific source of systematic errors on the astrometry. A major new aspect of *Gaia* DR4 is that it will include all time series data, that is, epoch astrometry, broad band photometry, radial velocities, and epoch BP, RP, and RVS spectra for all sources. In addition, we plan to release full astrometric, photometric, and radial-velocity catalogues; all the available variable-star and NSS solutions; an extended sample of source classifications and multiple APs for stars, and extragalactic objects. Finally, an updated extra-solar planet list will be published. The publication of *Gaia* DR4 is expected not before the end of 2025. *Gaia* DR5 will be the final release from the *Gaia* mission, and will be based on data collected over the full nominal plus extended mission periods and including all the data products mentioned above, as well as the *Gaia* legacy archive. *Gaia* DR5 is expected not before the end of 2030.

Figure 2 summarises the astrometric uncertainties of the *Gaia* data releases so far and also shows the extrapolated uncertainties for *Gaia* DR4 and *Gaia* DR5. The latter are extrapolated from the *Gaia* DR3 performance according to the amount of data collected, 5.5 years and an expected 10 years, respectively²⁶. With time the signal-to-noise ratio for all *Gaia* data products, including parallaxes, improves as \sqrt{t} , and therefore the precisions for *Gaia* DR4 and *Gaia* DR5 are expected to improve by factors of 1.4 and 1.9, respectively. For the proper motions, the improvement goes as $t^{1.5}$, which means improvements by factors of 2.7 and 6.6 with respect to *Gaia* DR3. For a more extensive discussion of the expected gains in future *Gaia* data releases, we refer to *Brown (2021)*.

There is therefore still much more to look forward to, but for now we invite the reader to explore the veritable supermarket of astronomical and astrophysical information that is *Gaia* DR3.

²⁵ software tools and the related documentation are available at <https://www.cosmos.esa.int/web/gaia/dr3-software-tools>

²⁶ <https://www.cosmos.esa.int/web/gaia/science-performance>

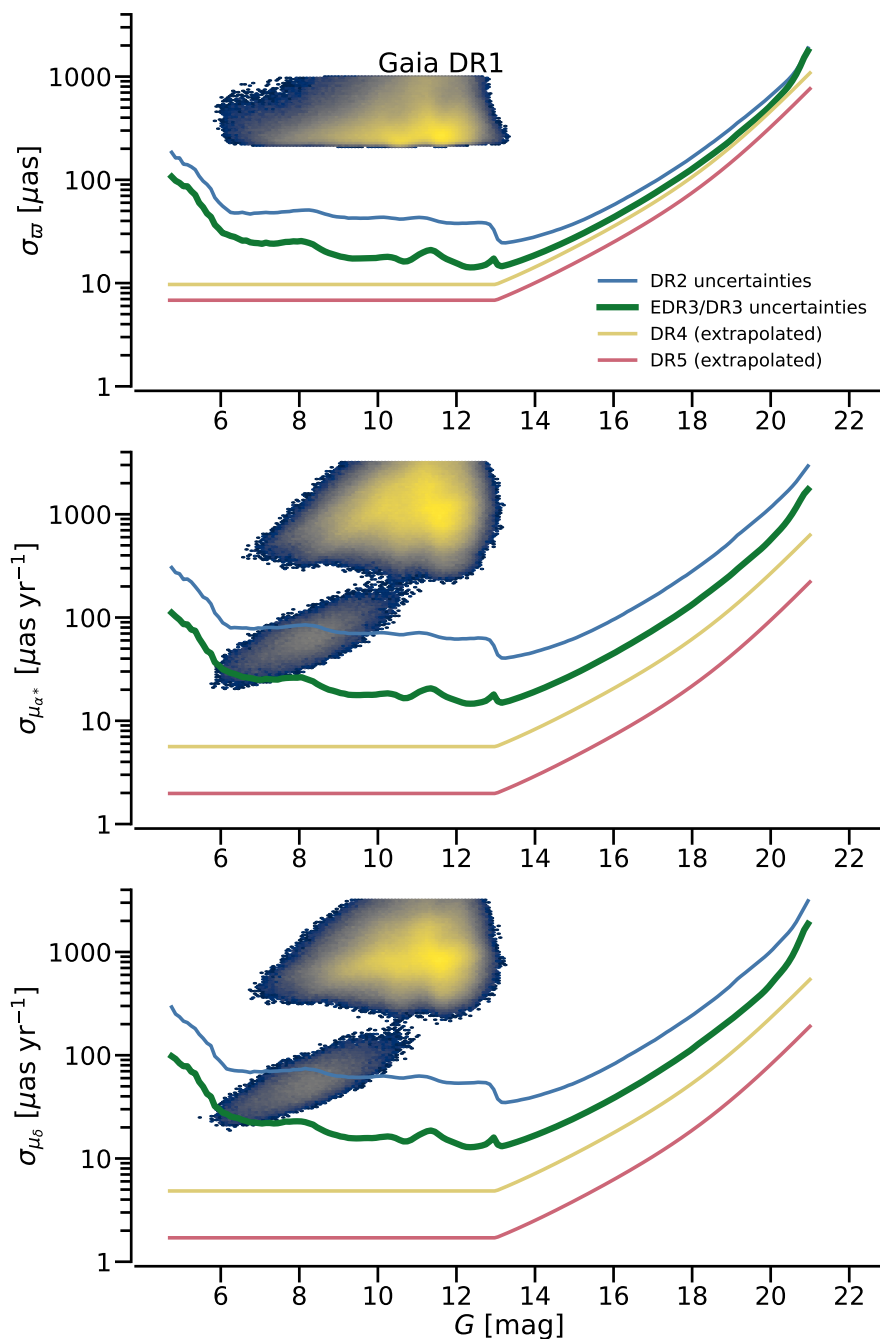


Fig. 2. Uncertainties on the astrometric parameters vs. G for *Gaia* data releases 1–3 and for the future releases *Gaia* DR4 and *Gaia* DR5. The panels show from top to bottom the uncertainties in parallax, proper motion in Right Ascension, and proper motion in Declination. The uncertainties for *Gaia* DR1 refer to the Tycho-*Gaia* Astrometric Solution and are shown in the form of density maps, with lighter colours indicating a higher density of sources. The two distinct low-uncertainty elliptical regions in the *Gaia* DR1 proper motion uncertainties are due to stars for which the *Hipparcos* and *Gaia* positions could be combined to derive proper motions over a 24-year time baseline. The proper motion uncertainties for *Gaia* DR3, based on only a 34 month time baseline are comparable or even slightly better.

Acknowledgements

This work presents results from the European Space Agency (ESA) space mission *Gaia*. *Gaia* data are being processed by the *Gaia* Data Processing and Analysis Consortium (DPAC). Funding for the DPAC is provided by national institutions, in particular the institutions participating in the *Gaia* MultiLateral Agreement (MLA). The *Gaia* mission website is <https://www.cosmos.esa.int/gaia>. The *Gaia* archive website is <https://archives.esac.esa.int/gaia>. Acknowledgements are given in Appendix A

References

- Ahn, C. P., Alexandroff, R., Allende Prieto, C., et al. 2012, *ApJS*, 203, 21
 Albareti, F. D., Allende Prieto, C., Almeida, A., et al. 2017, *ApJS*, 233, 25
 Andrae, R., Fouesneau, M., Sordo, R., Bailer-Jones, C., & et al. 2022, *A&A*, submitted
 Astropy Collaboration, Price-Whelan, A., Sipőcz, B. M., et al. 2018, *AJ*, 156, 123
 Babusiaux, C., Fabricius, C., & et al. 2022, *A&A*, submitted
 Blomme, R., Frémat, Y., Sartoretti, P., Guerrier, A., & et al. 2022, *A&A*, submitted
 Boch, T. & Fernique, P. 2014, in *Astronomical Society of the Pacific Conference Series*, Vol. 485, *Astronomical Data Analysis Software and Systems XXIII*, ed. N. Manset & P. Forshay, 277
 Bonnarel, F., Fernique, P., Bienaymé, O., et al. 2000, *A&AS*, 143, 33
 Breddels, M. A. & Veljanoski, J. 2018, *A&A*, 618, A13
 Brown, A. G. A. 2021, *ARA&A*, 59 [arXiv:2102.11712]
 Cantat-Gaudin, T. & Brandt, T. D. 2021, *A&A*, 649, A124
 Carnerero, M., Raiteri, C., Rimoldini, L., & Busonero, D. 2022, *A&A*, in prep.
 Carrasco, J. M., Weiler, M., Jordi, C., et al. 2021, *A&A*, 652, A86
 Chambers, K. C., Magnier, E. A., Metcalfe, N., et al. 2016, *ArXiv e-prints* [arXiv:1612.05560]
 Clementini, G., V. Ripepi, V., Garofalo, A., et al. 2022, *A&A*, in prep.

- Creevey, O., Sordo, R., Pailler, F., et al. 2022, A&A, submitted
- Cutri, R. M., Skrutskie, M. F., van Dyk, S., et al. 2013, *VizieR Online Data Catalogue*, 2328
- Damerdj, Y., Gosset, E., & et al. 2022, A&A, in prep.
- De Angeli, F., Weiler, M., Montegriffo, P., & et al. 2022, A&A, submitted
- de Bruijne, J. H. J., Allen, M., Azaz, S., et al. 2015, A&A, 576, A74
- Delchambre, L., Bailer-Jones, C., Bellas-Velidis, I., Drimmel, R., & et al. 2022, A&A, submitted
- Distefano, E., Lanzafame, A., & et al. 2022, A&A, in prep.
- Ducourant, C., Krone-Martins, A., Galluccio, L., Teixeira, R., & et al. 2022, A&A, submitted
- El-Badry, K., Rix, H.-W., & Heintz, T. M. 2021, MNRAS, 506, 2269
- Evans, D., Eyer, L., & et al. 2022, A&A, in prep.
- Eyer, L., Audard, M., Holl, B., & et al. 2022, A&A, in prep.
- Fabricius, C., Høg, E., Makarov, V. V., et al. 2002, A&A, 384, 180
- Fabricius, C., Luri, X., Arenou, F., et al. 2021, A&A, 649, A5
- Flewelling, H. A., Magnier, E. A., Chambers, K. C., et al. 2020, ApJS, 251, 7
- Flynn, C., Sekhri, R., Venville, T., et al. 2022, MNRAS, 509, 4276
- Fouesneau, M., Frémat, Y., Andrae, R., Korn, A., & et al. 2022, A&A, in prep.
- Frémat, Y., Royer, F., Marchal, O., Blomme, R., & et al. 2022, A&A, in prep.
- Gaia Collaboration, Arenou, F., Babusiaux, C., Barstow, M., & et al. 2022, A&A, submitted
- Gaia Collaboration, Bailer-Jones, C., Teyssier, D., Delchambre, L., & et al. 2022, A&A, accepted
- Gaia Collaboration, Brown, A. G. A., Vallenari, A., Prusti, T., et al. 2021, A&A, 649, A1
- Gaia Collaboration, Creevey, O., Sarro, L., Lobel, A., & et al. 2022, A&A, submitted
- Gaia Collaboration, De Ridder, J., Ripepi, V., Aerts, C., & et al. 2022, A&A, submitted
- Gaia Collaboration, Drimmel, R., Romero-Gomez, M., Chemin, L., & et al. 2022, A&A, in prep.
- Gaia Collaboration, Galluccio, L., Delbo, M., De Angeli, F., & et al. 2022, A&A, submitted
- Gaia Collaboration, Klioner, S. A., Lindegren, L., Mignard, F., & et al. 2022, arXiv e-prints, arXiv:2204.12574
- Gaia Collaboration, Montegriffo, P., Bellazzini, M., De Angeli, F., & et al. 2022, A&A, submitted
- Gaia Collaboration, Prusti, T., de Bruijne, J., Brown, A., et al. 2016, A&A, 595, A1
- Gaia Collaboration, Recio-Blanco, A., Kordopatis, G., de Laverny, P., & et al. 2022, A&A, submitted
- Gaia Collaboration, Schultheis, M., Zhao, H., Zwitter, T., & et al. 2022, A&A, accepted
- Gilmore, G., Randich, S., Worley, C. C., et al. 2022, A&A in press
- Gomel, R., Mazeh, T., Faigler, S., et al. 2022, A&A, submitted
- Gosset, E., Arenou, F., & et al. 2022, A&A in prep.
- Groenewegen, M. A. T. 2021, A&A, 654, A20
- Halbwachs, J.-L., Pourbaix¹, D., Arenou, F., Galluccio, L., & et al. 2022, A&A, in prep.
- Henden, A. A., Templeton, M., Terrell, D., et al. 2016, *VizieR Online Data Catalogue*, 2336
- Hodgkin, S. T., Harrison, D. L., Breedt, E., et al. 2021, A&A, 652, A76
- Høg, E., Fabricius, C., Makarov, V. V., et al. 2000, A&A, 355, L27
- Holl, B., Eyer, L., & et al. 2022, A&A, in prep.
- Huang, Y., Yuan, H., Beers, T. C., & Zhang, H. 2021, ApJ, 910, L5
- Huber, D., Bryson, S. T., Haas, M. R., et al. 2016, ApJS, 224, 2
- Hunter, J. D. 2007, *Computing In Science & Engineering*, 9, 90
- Katz, D., Sartoretti, P., & et al. 2022, A&A, in prep.
- Kohonen, T. 2001, *Self-Organizing Maps*, 3rd edn., Springer Series in Information Sciences (Berlin Heidelberg: Springer-Verlag)
- Kovacs, G. & Karamichucham, B. 2021, A&A, 653, A61
- Krone-Martins, A., Gavras, P., Ducourant, C., et al. 2022, A&A in prep.
- Lanzafame, A., Brugaletta, E., Frémat, Y., Sordo, R., & et al. 2022, A&A, in prep.
- Lasker, B. M., Lattanzi, M. G., McLean, B. J., et al. 2008, AJ, 136, 735
- Lebzelter, T., Mowlavi, N., & et al. 2022, A&A, in prep.
- Lindegren, L., Bastian, U., Biermann, M., et al. 2021a, A&A, 649, A4
- Lindegren, L., Klioner, S., Hernández, J., et al. 2021b, A&A, 649, A2
- Lunz, S., Anderson, J., Xu, M. H., et al. 2021, in EGU General Assembly Conference Abstracts, EGU General Assembly Conference Abstracts, EGU21–8604
- Luo, A. L., Zhao, Y.-H., Zhao, G., et al. 2015, *Research in Astronomy and Astrophysics*, 15, 1095
- Magnier, E. A., Chambers, K. C., Flewelling, H. A., et al. 2020a, ApJS, 251, 3
- Magnier, E. A., Schlafly, E. F., Finkbeiner, D. P., et al. 2020b, ApJS, 251, 6
- Magnier, E. A., Sweeney, W. E., Chambers, K. C., et al. 2020c, ApJS, 251, 5
- Maíz Apellániz, J. 2022, A&A, 657, A130
- Maíz Apellániz, J., Pantaleoni González, M., & Barbá, R. H. 2021, A&A, 649, A13
- Marton, G., Kun, M., Ábrahám, P., Szabados, L., & et al. 2022, A&A, in prep.
- Molnar, T. A., Sanders, J. L., Smith, L. C., et al. 2022, MNRAS, 509, 2566
- Montegriffo, P., De Angeli, F., Andrae, R., Riello, M., & et al. 2022, A&A, submitted
- Mowlavi, N., Holl, B., & et al. 2022, A&A, in prep.
- Niu, Z., Yuan, H., & Liu, J. 2021, ApJ, 908, L14
- Ochsenbein, F., Bauer, P., & Marcout, J. 2000, A&AS, 143, 23
- Onken, C. A., Wolf, C., Bessell, M. S., et al. 2019, PASA, 36, e033
- Panahi, A., Zucker, S., Clementini, G., Audard, M., & et al. 2022, A&A, submitted
- Pancino, E., Sanna, N., Altavilla, G., et al. 2021a, MNRAS, 503, 3660
- Pancino, E., Sanna, N., Altavilla, G., et al. 2021b, MNRAS, 503, 3660
- Pérez, F. & Granger, B. E. 2007, *Computing in Science and Engineering*, 9, 21
- R Core Team. 2013, *R: A Language and Environment for Statistical Computing*, R Foundation for Statistical Computing, Vienna, Austria
- Randich, S., Gilmore, G., Magrini, L., et al. 2022, A&A in press
- Recio-Blanco, A., de Laverny, P., Palicio, P., Kordopatis, G., & et al. 2022, A&A submitted
- Ren, F., Chen, X., Zhang, H., et al. 2021, ApJ, 911, L20
- Riello, M., De Angeli, F., Evans, D. W., et al. 2021, A&A, 649, A3
- Riess, A. G., Casertano, S., Yuan, W., et al. 2021, ApJ, 908, L6
- Rimoldini, L., Holl, B., Audard, M., et al. 2019, A&A, 625, A97
- Ripepi, V., Clementini, G., & et al. 2022, A&A, in prep.
- Robin, A. C., Luri, X., Reylé, C., et al. 2012, A&A, 543, A100
- Roeser, S., Demleitner, M., & Schilbach, E. 2010, AJ, 139, 2440
- Rowell, N., Davidson, M., Lindegren, L., et al. 2021, A&A, 649, A11
- Sartoretti, P., Blomme, R., David, M., & Seabroke, G. 2022a, Gaia DR3 documentation Chapter 6: Spectroscopy, Gaia DR3 documentation
- Sartoretti, P., Marchal, O., Babusiaux, C., Jordi, C., & et al. 2022b, A&A, submitted
- Seabroke, G., Sartoretti, P., & et al. 2022, A&A, in prep.
- Seabroke, G. M., Fabricius, C., Teyssier, D., et al. 2021, A&A, 653, A160
- Siopis, C., Pourbaix, D., & et al. 2022, A&A in prep.
- Skutskie, M. F., Cutri, R. M., Stiening, R., et al. 2006, AJ, 131, 1163
- Stassun, K. G. & Torres, G. 2021, ApJ, 907, L33
- Steinmetz, M., Guiglion, G., McMillan, P. J., et al. 2020a, AJ, 160, 83
- Steinmetz, M., Matijević, G., Enke, H., et al. 2020b, AJ, 160, 82
- Tanga, P., Pauwels, T., Mignard, F., Muinonen, K., & et al. 2022, A&A, submitted
- Taylor, M. B. 2005, in *Astronomical Society of the Pacific Conference Series*, Vol. 347, *Astronomical Data Analysis Software and Systems XIV*, ed. P. Shopbell, M. Britton, & R. Ebert, 29
- Taylor, M. B. 2006, in *Astronomical Society of the Pacific Conference Series*, Vol. 351, *Astronomical Data Analysis Software and Systems XV*, ed. C. Gabriel, C. Arviset, D. Ponz, & S. Enrique, 666
- Thanjavur, K., Ivezić, Ž., Allam, S. S., et al. 2021, MNRAS, 505, 5941
- Torra, F., Castañeda, J., Fabricius, C., et al. 2021, A&A, 649, A10
- Torres, F. 2007, A&A, 474, 653
- Vasiliev, E. & Baumgardt, H. 2021, MNRAS, 505, 5978
- Wang, C., Yuan, H., & Huang, Y. 2022, AJ, 163, 149
- Waters, C. Z., Magnier, E. A., Price, P. A., et al. 2020, ApJS, 251, 4
- Wenger, M., Ochsenbein, F., Egret, D., et al. 2000, A&AS, 143, 9
- Wyrzykowski, Ł., Kruszyńska, K., Rybicki, K., Holl, B., & et al. 2022, A&A, submitted
- Yang, L., Yuan, H., Zhang, R., et al. 2021, ApJ, 908, L24
- Zacharias, N., Finch, C., Subasavage, J., et al. 2015, AJ, 150, 101
- Zacharias, N., Finch, C. T., Girard, T. M., et al. 2013, AJ, 145, 44
- Zinn, J. C. 2021, AJ, 161, 214

¹ INAF - Osservatorio astronomico di Padova, Vicolo Osservatorio 5, 35122 Padova, Italy

² Leiden Observatory, Leiden University, Niels Bohrweg 2, 2333 CA Leiden, The Netherlands

³ European Space Agency (ESA), European Space Research and Technology Centre (ESTEC), Keplerlaan 1, 2201AZ, Noordwijk, The Netherlands

⁴ GEPI, Observatoire de Paris, Université PSL, CNRS, 5 Place Jules Janssen, 92190 Meudon, France

⁵ Univ. Grenoble Alpes, CNRS, IPAG, 38000 Grenoble, France

⁶ Astronomisches Rechen-Institut, Zentrum für Astronomie der Universität Heidelberg, Mönchhofstr. 12-14, 69120 Heidelberg, Germany

⁷ Université Côte d'Azur, Observatoire de la Côte d'Azur, CNRS, Laboratoire Lagrange, Bd de l'Observatoire, CS 34229, 06304 Nice Cedex 4, France

⁸ Laboratoire d'astrophysique de Bordeaux, Univ. Bordeaux, CNRS, B18N, allée Geoffroy Saint-Hilaire, 33615 Pessac, France

- ⁹ Institute of Astronomy, University of Cambridge, Madingley Road, Cambridge CB3 0HA, United Kingdom
- ¹⁰ Department of Astronomy, University of Geneva, Chemin Pegasi 51, 1290 Versoix, Switzerland
- ¹¹ European Space Agency (ESA), European Space Astronomy Centre (ESAC), Camino bajo del Castillo, s/n, Urbanizacion Villafranca del Castillo, Villanueva de la Cañada, 28692 Madrid, Spain
- ¹² Aurora Technology for European Space Agency (ESA), Camino bajo del Castillo, s/n, Urbanizacion Villafranca del Castillo, Villanueva de la Cañada, 28692 Madrid, Spain
- ¹³ Institut de Ciències del Cosmos (ICCUB), Universitat de Barcelona (IEEC-UB), Martí i Franquès 1, 08028 Barcelona, Spain
- ¹⁴ Lohrmann Observatory, Technische Universität Dresden, Mommsenstraße 13, 01062 Dresden, Germany
- ¹⁵ Lund Observatory, Department of Astronomy and Theoretical Physics, Lund University, Box 43, 22100 Lund, Sweden
- ¹⁶ CNES Centre Spatial de Toulouse, 18 avenue Edouard Belin, 31401 Toulouse Cedex 9, France
- ¹⁷ Institut d'Astronomie et d'Astrophysique, Université Libre de Bruxelles CP 226, Boulevard du Triomphe, 1050 Brussels, Belgium
- ¹⁸ F.R.S.-FNRS, Rue d'Egmont 5, 1000 Brussels, Belgium
- ¹⁹ INAF - Osservatorio Astrofisico di Arcetri, Largo Enrico Fermi 5, 50125 Firenze, Italy
- ²⁰ Max Planck Institute for Astronomy, Königstuhl 17, 69117 Heidelberg, Germany
- ²¹ INAF - Osservatorio Astrofisico di Torino, via Osservatorio 20, 10025 Pino Torinese (TO), Italy
- ²² European Space Agency (ESA, retired)
- ²³ University of Turin, Department of Physics, Via Pietro Giuria 1, 10125 Torino, Italy
- ²⁴ INAF - Osservatorio di Astrofisica e Scienza dello Spazio di Bologna, via Piero Gobetti 93/3, 40129 Bologna, Italy
- ²⁵ DAPCOM for Institut de Ciències del Cosmos (ICCUB), Universitat de Barcelona (IEEC-UB), Martí i Franquès 1, 08028 Barcelona, Spain
- ²⁶ Royal Observatory of Belgium, Ringlaan 3, 1180 Brussels, Belgium
- ²⁷ Observational Astrophysics, Division of Astronomy and Space Physics, Department of Physics and Astronomy, Uppsala University, Box 516, 751 20 Uppsala, Sweden
- ²⁸ ALTEC S.p.a, Corso Marche, 79,10146 Torino, Italy
- ²⁹ Sàrl, Geneva, Switzerland
- ³⁰ Department of Astronomy, University of Geneva, Chemin d'Ecogia 16, 1290 Versoix, Switzerland
- ³¹ Mullard Space Science Laboratory, University College London, Holmbury St Mary, Dorking, Surrey RH5 6NT, United Kingdom
- ³² Gaia DPAC Project Office, ESAC, Camino bajo del Castillo, s/n, Urbanizacion Villafranca del Castillo, Villanueva de la Cañada, 28692 Madrid, Spain
- ³³ Telespazio UK S.L. for European Space Agency (ESA), Camino bajo del Castillo, s/n, Urbanizacion Villafranca del Castillo, Villanueva de la Cañada, 28692 Madrid, Spain
- ³⁴ SYRTE, Observatoire de Paris, Université PSL, CNRS, Sorbonne Université, LNE, 61 avenue de l'Observatoire 75014 Paris, France
- ³⁵ National Observatory of Athens, I. Metaxa and Vas. Pavlou, Palaia Penteli, 15236 Athens, Greece
- ³⁶ IMCCE, Observatoire de Paris, Université PSL, CNRS, Sorbonne Université, Univ. Lille, 77 av. Denfert-Rochereau, 75014 Paris, France
- ³⁷ Serco Gestión de Negocios for European Space Agency (ESA), Camino bajo del Castillo, s/n, Urbanizacion Villafranca del Castillo, Villanueva de la Cañada, 28692 Madrid, Spain
- ³⁸ Institut d'Astrophysique et de Géophysique, Université de Liège, 19c, Allée du 6 Août, B-4000 Liège, Belgium
- ³⁹ CRAAG - Centre de Recherche en Astronomie, Astrophysique et Géophysique, Route de l'Observatoire Bp 63 Bouzareah 16340 Algiers, Algeria
- ⁴⁰ Institute for Astronomy, University of Edinburgh, Royal Observatory, Blackford Hill, Edinburgh EH9 3HJ, United Kingdom
- ⁴¹ RHEA for European Space Agency (ESA), Camino bajo del Castillo, s/n, Urbanizacion Villafranca del Castillo, Villanueva de la Cañada, 28692 Madrid, Spain
- ⁴² ATG Europe for European Space Agency (ESA), Camino bajo del Castillo, s/n, Urbanizacion Villafranca del Castillo, Villanueva de la Cañada, 28692 Madrid, Spain
- ⁴³ CIGUS CITIC - Department of Computer Science and Information Technologies, University of A Coruña, Campus de Elviña s/n, A Coruña, 15071, Spain
- ⁴⁴ Université de Strasbourg, CNRS, Observatoire astronomique de Strasbourg, UMR 7550, 11 rue de l'Université, 67000 Strasbourg, France
- ⁴⁵ Kavli Institute for Cosmology Cambridge, Institute of Astronomy, Madingley Road, Cambridge, CB3 0HA
- ⁴⁶ Leibniz Institute for Astrophysics Potsdam (AIP), An der Sternwarte 16, 14482 Potsdam, Germany
- ⁴⁷ CENTRA, Faculdade de Ciências, Universidade de Lisboa, Edif. C8, Campo Grande, 1749-016 Lisboa, Portugal
- ⁴⁸ Department of Informatics, Donald Bren School of Information and Computer Sciences, University of California, Irvine, 5226 Donald Bren Hall, 92697-3440 CA Irvine, United States
- ⁴⁹ INAF - Osservatorio Astrofisico di Catania, via S. Sofia 78, 95123 Catania, Italy
- ⁵⁰ Dipartimento di Fisica e Astronomia ""Ettore Majorana"", Università di Catania, Via S. Sofia 64, 95123 Catania, Italy
- ⁵¹ INAF - Osservatorio Astronomico di Roma, Via Frascati 33, 00078 Monte Porzio Catone (Roma), Italy
- ⁵² Space Science Data Center - ASI, Via del Politecnico SNC, 00133 Roma, Italy
- ⁵³ Department of Physics, University of Helsinki, P.O. Box 64, 00014 Helsinki, Finland
- ⁵⁴ Finnish Geospatial Research Institute FGI, Geodeetinrinne 2, 02430 Masala, Finland
- ⁵⁵ Institut UTINAM CNRS UMR6213, Université Bourgogne Franche-Comté, OSU THETA Franche-Comté Bourgogne, Observatoire de Besançon, BP1615, 25010 Besançon Cedex, France
- ⁵⁶ HE Space Operations BV for European Space Agency (ESA), Keplerlaan 1, 2201AZ, Noordwijk, The Netherlands
- ⁵⁷ Dpto. de Inteligencia Artificial, UNED, c/ Juan del Rosal 16, 28040 Madrid, Spain
- ⁵⁸ Konkoly Observatory, Research Centre for Astronomy and Earth Sciences, Eötvös Loránd Research Network (ELKH), MTA Centre of Excellence, Konkoly Thege Miklós út 15-17, 1121 Budapest, Hungary
- ⁵⁹ ELTE Eötvös Loránd University, Institute of Physics, 1117, Pázmány Péter sétány 1A, Budapest, Hungary
- ⁶⁰ Instituut voor Sterrenkunde, KU Leuven, Celestijnenlaan 200D, 3001 Leuven, Belgium
- ⁶¹ Department of Astrophysics/IMAPP, Radboud University, P.O.Box 9010, 6500 GL Nijmegen, The Netherlands
- ⁶² University of Vienna, Department of Astrophysics, Türkenschanzstraße 17, A1180 Vienna, Austria
- ⁶³ Institute of Physics, Laboratory of Astrophysics, Ecole Polytechnique Fédérale de Lausanne (EPFL), Observatoire de Sauverny, 1290 Versoix, Switzerland
- ⁶⁴ Kapteyn Astronomical Institute, University of Groningen, Landlevan 12, 9747 AD Groningen, The Netherlands
- ⁶⁵ School of Physics and Astronomy / Space Park Leicester, University of Leicester, University Road, Leicester LE1 7RH, United Kingdom
- ⁶⁶ Thales Services for CNES Centre Spatial de Toulouse, 18 avenue Edouard Belin, 31401 Toulouse Cedex 9, France
- ⁶⁷ Depto. Estadística e Investigación Operativa. Universidad de Cádiz, Avda. República Saharaui s/n, 11510 Puerto Real, Cádiz, Spain
- ⁶⁸ Center for Research and Exploration in Space Science and Technology, University of Maryland Baltimore County, 1000 Hilltop Circle, Baltimore MD, USA
- ⁶⁹ GSFC - Goddard Space Flight Center, Code 698, 8800 Greenbelt Rd, 20771 MD Greenbelt, United States
- ⁷⁰ EURIX S.r.l., Corso Vittorio Emanuele II 61, 10128, Torino, Italy

- 71 Porter School of the Environment and Earth Sciences, Tel Aviv University, Tel Aviv 6997801, Israel
- 72 Harvard-Smithsonian Center for Astrophysics, 60 Garden St., MS 15, Cambridge, MA 02138, USA
- 73 ATOS for CNES Centre Spatial de Toulouse, 18 avenue Edouard Belin, 31401 Toulouse Cedex 9, France
- 74 HE Space Operations BV for European Space Agency (ESA), Camino bajo del Castillo, s/n, Urbanizacion Villafranca del Castillo, Villanueva de la Cañada, 28692 Madrid, Spain
- 75 Instituto de Astrofísica e Ciências do Espaço, Universidade do Porto, CAUP, Rua das Estrelas, PT4150-762 Porto, Portugal
- 76 LFCA/DAS, Universidad de Chile, CNRS, Casilla 36-D, Santiago, Chile
- 77 SISSA - Scuola Internazionale Superiore di Studi Avanzati, via Bonomea 265, 34136 Trieste, Italy
- 78 Telespazio for CNES Centre Spatial de Toulouse, 18 avenue Edouard Belin, 31401 Toulouse Cedex 9, France
- 79 University of Turin, Department of Computer Sciences, Corso Svizzera 185, 10149 Torino, Italy
- 80 Dpto. de Matemática Aplicada y Ciencias de la Computación, Univ. de Cantabria, ETS Ingenieros de Caminos, Canales y Puertos, Avda. de los Castros s/n, 39005 Santander, Spain
- 81 Centro de Astronomía - CITEVA, Universidad de Antofagasta, Avenida Angamos 601, Antofagasta 1270300, Chile
- 82 DLR Gesellschaft für Raumfahrtanwendungen (GfR) mbH Münchener Straße 20, 82234 Weßling
- 83 Centre for Astrophysics Research, University of Hertfordshire, College Lane, AL10 9AB, Hatfield, United Kingdom
- 84 University of Turin, Mathematical Department "G. Peano", Via Carlo Alberto 10, 10123 Torino, Italy
- 85 University of Antwerp, Onderzoeksgroep Toegepaste Wiskunde, Middelheimlaan 1, 2020 Antwerp, Belgium
- 86 INAF - Osservatorio Astronomico d'Abruzzo, Via Mentore Maggini, 64100 Teramo, Italy
- 87 Instituto de Astronomia, Geofísica e Ciências Atmosféricas, Universidade de São Paulo, Rua do Matão, 1226, Cidade Universitária, 05508-900 São Paulo, SP, Brazil
- 88 APAVE SUDEUROPE SAS for CNES Centre Spatial de Toulouse, 18 avenue Edouard Belin, 31401 Toulouse Cedex 9, France
- 89 Mésocentre de calcul de Franche-Comté, Université de Franche-Comté, 16 route de Gray, 25030 Besançon Cedex, France
- 90 Theoretical Astrophysics, Division of Astronomy and Space Physics, Department of Physics and Astronomy, Uppsala University, Box 516, 751 20 Uppsala, Sweden
- 91 School of Physics and Astronomy, Tel Aviv University, Tel Aviv 6997801, Israel
- 92 Astrophysics Research Centre, School of Mathematics and Physics, Queen's University Belfast, Belfast BT7 1NN, UK
- 93 Centre de Données Astronomiques de Strasbourg, Strasbourg, France
- 94 Université Côte d'Azur, Observatoire de la Côte d'Azur, CNRS, Laboratoire Géoazur, Bd de l'Observatoire, CS 34229, 06304 Nice Cedex 4, France
- 95 Institute for Computational Cosmology, Department of Physics, Durham University, Durham DH1 3LE, UK
- 96 European Southern Observatory, Karl-Schwarzschild-Str. 2, 85748 Garching, Germany
- 97 Max-Planck-Institut für Astrophysik, Karl-Schwarzschild-Straße 1, 85748 Garching, Germany
- 98 Data Science and Big Data Lab, Pablo de Olavide University, 41013, Seville, Spain
- 99 Barcelona Supercomputing Center (BSC), Plaça Eusebi Güell 1-3, 08034-Barcelona, Spain
- 100 ETSE Telecomunicación, Universidade de Vigo, Campus Lagoas-Marcosende, 36310 Vigo, Galicia, Spain
- 101 Asteroid Engineering Laboratory, Space Systems, Luleå University of Technology, Box 848, S-981 28 Kiruna, Sweden
- 102 Vera C Rubin Observatory, 950 N. Cherry Avenue, Tucson, AZ 85719, USA
- 103 Department of Astrophysics, Astronomy and Mechanics, National and Kapodistrian University of Athens, Panepistimiopolis, Zografos, 15783 Athens, Greece
- 104 TRUMPF Photonic Components GmbH, Lise-Meitner-Straße 13, 89081 Ulm, Germany
- 105 IAC - Instituto de Astrofísica de Canarias, Via Láctea s/n, 38200 La Laguna S.C., Tenerife, Spain
- 106 Department of Astrophysics, University of La Laguna, Via Láctea s/n, 38200 La Laguna S.C., Tenerife, Spain
- 107 Faculty of Aerospace Engineering, Delft University of Technology, Kluyverweg 1, 2629 HS Delft, The Netherlands
- 108 Radagast Solutions
- 109 Laboratoire Univers et Particules de Montpellier, CNRS Université Montpellier, Place Eugène Bataillon, CC72, 34095 Montpellier Cedex 05, France
- 110 Université de Caen Normandie, Côte de Nacre Boulevard Maréchal Juin, 14032 Caen, France
- 111 LESIA, Observatoire de Paris, Université PSL, CNRS, Sorbonne Université, Université de Paris, 5 Place Jules Janssen, 92190 Meudon, France
- 112 SRON Netherlands Institute for Space Research, Niels Bohrweg 4, 2333 CA Leiden, The Netherlands
- 113 Astronomical Observatory, University of Warsaw, Al. Ujazdowskie 4, 00-478 Warszawa, Poland
- 114 Scialia for CNES Centre Spatial de Toulouse, 18 avenue Edouard Belin, 31401 Toulouse Cedex 9, France
- 115 Université Rennes, CNRS, IPR (Institut de Physique de Rennes) - UMR 6251, 35000 Rennes, France
- 116 INAF - Osservatorio Astronomico di Capodimonte, Via Moiriello 16, 80131, Napoli, Italy
- 117 Shanghai Astronomical Observatory, Chinese Academy of Sciences, 80 Nandan Road, Shanghai 200030, People's Republic of China
- 118 University of Chinese Academy of Sciences, No.19(A) Yuquan Road, Shijingshan District, Beijing 100049, People's Republic of China
- 119 Niels Bohr Institute, University of Copenhagen, Juliane Maries Vej 30, 2100 Copenhagen Ø, Denmark
- 120 DXC Technology, Retortvej 8, 2500 Valby, Denmark
- 121 Las Cumbres Observatory, 6740 Cortona Drive Suite 102, Goleta, CA 93117, USA
- 122 CIGUS CITIC, Department of Nautical Sciences and Marine Engineering, University of A Coruña, Paseo de Ronda 51, 15071, A Coruña, Spain
- 123 Astrophysics Research Institute, Liverpool John Moores University, 146 Brownlow Hill, Liverpool L3 5RF, United Kingdom
- 124 IPAC, Mail Code 100-22, California Institute of Technology, 1200 E. California Blvd., Pasadena, CA 91125, USA
- 125 IRAP, Université de Toulouse, CNRS, UPS, CNES, 9 Av. colonel Roche, BP 44346, 31028 Toulouse Cedex 4, France
- 126 MTA CSFK Lendület Near-Field Cosmology Research Group, Konkoly Observatory, MTA Research Centre for Astronomy and Earth Sciences, Konkoly Thege Miklós út 15-17, 1121 Budapest, Hungary
- 127 Departamento de Física de la Tierra y Astrofísica, Universidad Complutense de Madrid, 28040 Madrid, Spain
- 128 Ruđer Bošković Institute, Bijenička cesta 54, 10000 Zagreb, Croatia
- 129 Villanova University, Department of Astrophysics and Planetary Science, 800 E Lancaster Avenue, Villanova PA 19085, USA
- 130 INAF - Osservatorio Astronomico di Brera, via E. Bianchi, 46, 23807 Merate (LC), Italy
- 131 STFC, Rutherford Appleton Laboratory, Harwell, Didcot, OX11 0QX, United Kingdom
- 132 Charles University, Faculty of Mathematics and Physics, Astronomical Institute of Charles University, V Holesovickach 2, 18000 Prague, Czech Republic
- 133 Department of Particle Physics and Astrophysics, Weizmann Institute of Science, Rehovot 7610001, Israel

- ¹³⁴ Department of Astrophysical Sciences, 4 Ivy Lane, Princeton University, Princeton NJ 08544, USA
- ¹³⁵ Departamento de Astrofísica, Centro de Astrobiología (CSIC-INTA), ESA-ESAC. Camino Bajo del Castillo s/n. 28692 Villanueva de la Cañada, Madrid, Spain
- ¹³⁶ naXys, University of Namur, Rempart de la Vierge, 5000 Namur, Belgium
- ¹³⁷ CGI Deutschland B.V. & Co. KG, Mornewegstr. 30, 64293 Darmstadt, Germany
- ¹³⁸ Institute of Global Health, University of Geneva
- ¹³⁹ Astronomical Observatory Institute, Faculty of Physics, Adam Mickiewicz University, Poznań, Poland
- ¹⁴⁰ H H Wills Physics Laboratory, University of Bristol, Tyndall Avenue, Bristol BS8 1TL, United Kingdom
- ¹⁴¹ Department of Physics and Astronomy G. Galilei, University of Padova, Vicolo dell'Osservatorio 3, 35122, Padova, Italy
- ¹⁴² CERN, Geneva, Switzerland
- ¹⁴³ Applied Physics Department, Universidade de Vigo, 36310 Vigo, Spain
- ¹⁴⁴ Association of Universities for Research in Astronomy, 1331 Pennsylvania Ave. NW, Washington, DC 20004, USA
- ¹⁴⁵ European Southern Observatory, Alonso de Córdova 3107, Casilla 19, Santiago, Chile
- ¹⁴⁶ Sorbonne Université, CNRS, UMR7095, Institut d'Astrophysique de Paris, 98bis bd. Arago, 75014 Paris, France
- ¹⁴⁷ Faculty of Mathematics and Physics, University of Ljubljana, Jadranska ulica 19, 1000 Ljubljana, Slovenia

Appendix A:

The *Gaia* mission and data processing have financially been supported by, in alphabetical order by country:

- the Algerian Centre de Recherche en Astronomie, Astrophysique et Géophysique of Bouzareah Observatory;
- the Austrian Fonds zur Förderung der wissenschaftlichen Forschung (FWF) Hertha Firnberg Programme through grants T359, P20046, and P23737;
- the BELgian federal Science Policy Office (BEL-SPO) through various PROgramme de Développement d’Expériences scientifiques (PRODEX) grants and the Polish Academy of Sciences - Fonds Wetenschappelijk Onderzoek through grant VS.091.16N, and the Fonds de la Recherche Scientifique (FNRS), and the Research Council of Katholieke Universiteit (KU) Leuven through grant C16/18/005 (Pushing AsteRoseismology to the next level with TESS, GaiA, and the Sloan Digital Sky SurVEy – PARADISE);
- the Brazil-France exchange programmes Fundação de Amparo à Pesquisa do Estado de São Paulo (FAPESP) and Coordenação de Aperfeiçoamento de Pessoal de Nível Superior (CAPES) - Comité Français d’Evaluation de la Coopération Universitaire et Scientifique avec le Brésil (COFECUB);
- the Chilean Agencia Nacional de Investigación y Desarrollo (ANID) through Fondo Nacional de Desarrollo Científico y Tecnológico (FONDECYT) Regular Project 1210992 (L. Chemin);
- the National Natural Science Foundation of China (NSFC) through grants 11573054, 11703065, and 12173069, the China Scholarship Council through grant 201806040200, and the Natural Science Foundation of Shanghai through grant 21ZR1474100;
- the Tenure Track Pilot Programme of the Croatian Science Foundation and the École Polytechnique Fédérale de Lausanne and the project TTP-2018-07-1171 ‘Mining the Variable Sky’, with the funds of the Croatian-Swiss Research Programme;
- the Czech-Republic Ministry of Education, Youth, and Sports through grant LG 15010 and INTER-EXCELLENCE grant LTAUSA18093, and the Czech Space Office through ESA PECS contract 98058;
- the Danish Ministry of Science;
- the Estonian Ministry of Education and Research through grant IUT40-1;
- the European Commission’s Sixth Framework Programme through the European Leadership in Space Astrometry (ELSA) Marie Curie Research Training Network (MRTN-CT-2006-033481), through Marie Curie project PIOFGA-2009-255267 (Space AsteroSeismology & RR Lyrae stars, SAS-RRL), and through a Marie Curie Transfer-of-Knowledge (ToK) fellowship (MTKD-CT-2004-014188); the European Commission’s Seventh Framework Programme through grant FP7-606740 (FP7-SPACE-2013-1) for the *Gaia* European Network for Improved data User Services (GENIUS) and through grant 264895 for the *Gaia* Research for European Astronomy Training (GREAT-ITN) network;
- the European Cooperation in Science and Technology (COST) through COST Action CA18104 ‘Revealing the Milky Way with *Gaia* (MW-Gaia)’;
- the European Research Council (ERC) through grants 320360, 647208, and 834148 and through the European Union’s Horizon 2020 research and innovation and excellent science programmes through Marie Skłodowska-Curie grant 745617 (Our Galaxy at full HD – Gal-HD) and 895174 (The build-up and fate of self-gravitating systems in the Universe) as well as grants 687378 (Small Bodies: Near and Far), 682115 (Using the Magellanic Clouds to Understand the Interaction of Galaxies), 695099 (A sub-percent distance scale from binaries and Cepheids – CepBin), 716155 (Structured ACCREtion Disks – SACCRED), 951549 (Sub-percent calibration of the extragalactic distance scale in the era of big surveys – UniverScale), and 101004214 (Innovative Scientific Data Exploration and Exploitation Applications for Space Sciences – EXPLORE);
- the European Science Foundation (ESF), in the framework of the *Gaia* Research for European Astronomy Training Research Network Programme (GREAT-ESF);
- the European Space Agency (ESA) in the framework of the *Gaia* project, through the Plan for European Cooperating States (PECS) programme through contracts C98090 and 4000106398/12/NL/KML for Hungary, through contract 4000115263/15/NL/IB for Germany, and through Programme de Développement d’Expériences scientifiques (PRODEX) grant 4000127986 for Slovenia;
- the Academy of Finland through grants 299543, 307157, 325805, 328654, 336546, and 345115 and the Magnus Ehrnrooth Foundation;
- the French Centre National d’Études Spatiales (CNES), the Agence Nationale de la Recherche (ANR) through grant ANR-10-IDEX-0001-02 for the ‘Investissements d’avenir’ programme, through grant ANR-15-CE31-0007 for project ‘Modelling the Milky Way in the *Gaia* era’ (MOD4Gaia), through grant ANR-14-CE33-0014-01 for project ‘The Milky Way disc formation in the *Gaia* era’ (ARCHEOGAL), through grant ANR-15-CE31-0012-01 for project ‘Unlocking the potential of Cepheids as primary distance calibrators’ (UnlockCepheids), through grant ANR-19-CE31-0017 for project ‘Secular evolution of galaxies’ (SEGAL), and through grant ANR-18-CE31-0006 for project ‘Galactic Dark Matter’ (GaDaMa), the Centre National de la Recherche Scientifique (CNRS) and its SNO *Gaia* of the Institut des Sciences de l’Univers (INSU), its Programmes Nationaux: Cosmologie et Galaxies (PNCG), Gravitation Références Astronomie Métrologie (PNGRAM), Planétologie (PNP), Physique et Chimie du Milieu Interstellaire (PCMI), and Physique Stellaire (PNPS), the ‘Action Fédératrice *Gaia*’ of the Observatoire de Paris, the Région de Franche-Comté, the Institut National Polytechnique (INP) and the Institut National de Physique nucléaire et de Physique des Particules (IN2P3) co-funded by CNES;
- the German Aerospace Agency (Deutsches Zentrum für Luft- und Raumfahrt e.V., DLR) through grants 50QG0501, 50QG0601, 50QG0602, 50QG0701, 50QG0901, 50QG1001, 50QG1101, 50QG1401, 50QG1402, 50QG1403, 50QG1404, 50QG1904, 50QG2101, 50QG2102, and 50QG2202, and the Centre for Information Services and High Performance Computing (ZIH) at the Technische Universität Dresden for generous allocations of computer time;
- the Hungarian Academy of Sciences through the Lendület Programme grants LP2014-17 and LP2018-7 and the Hungarian National Research, Development, and Innovation Office (NKFIH) through grant KKP-137523 (‘SeismoLab’);
- the Science Foundation Ireland (SFI) through a Royal Society - SFI University Research Fellowship (M. Fraser);

- the Israel Ministry of Science and Technology through grant 3-18143 and the Tel Aviv University Center for Artificial Intelligence and Data Science (TAD) through a grant;
 - the Agenzia Spaziale Italiana (ASI) through contracts I/037/08/0, I/058/10/0, 2014-025-R.0, 2014-025-R.1.2015, and 2018-24-HH.0 to the Italian Istituto Nazionale di Astrofisica (INAF), contract 2014-049-R.0/1/2 to INAF for the Space Science Data Centre (SSDC, formerly known as the ASI Science Data Center, ASDC), contracts I/008/10/0, 2013/030/I.0, 2013-030-I.0.1-2015, and 2016-17-I.0 to the Aerospace Logistics Technology Engineering Company (ALTEC S.p.A.), INAF, and the Italian Ministry of Education, University, and Research (Ministero dell’Istruzione, dell’Università e della Ricerca) through the Premiale project ‘Mining The Cosmos Big Data and Innovative Italian Technology for Frontier Astrophysics and Cosmology’ (MITiC);
 - the Netherlands Organisation for Scientific Research (NWO) through grant NWO-M-614.061.414, through a VICI grant (A. Helmi), and through a Spinoza prize (A. Helmi), and the Netherlands Research School for Astronomy (NOVA);
 - the Polish National Science Centre through HARMONIA grant 2018/30/M/ST9/00311 and DAINA grant 2017/27/L/ST9/03221 and the Ministry of Science and Higher Education (MNiSW) through grant DIR/WK/2018/12;
 - the Portuguese Fundação para a Ciência e a Tecnologia (FCT) through national funds, grants SFRH/BD/128840/2017 and PTDC/FIS-AST/30389/2017, and work contract DL 57/2016/CP1364/CT0006, the Fundo Europeu de Desenvolvimento Regional (FEDER) through grant POCI-01-0145-FEDER-030389 and its Programa Operacional Competitividade e Internacionalização (COMPETE2020) through grants UIDB/04434/2020 and UIDP/04434/2020, and the Strategic Programme UIDB/00099/2020 for the Centro de Astrofísica e Gravitação (CENTRA);
 - the Slovenian Research Agency through grant P1-0188;
 - the Spanish Ministry of Economy (MINECO/FEDER, UE), the Spanish Ministry of Science and Innovation (MICIN), the Spanish Ministry of Education, Culture, and Sports, and the Spanish Government through grants BES-2016-078499, BES-2017-083126, BES-C-2017-0085, ESP2016-80079-C2-1-R, ESP2016-80079-C2-2-R, FPU16/03827, PDC2021-121059-C22, RTI2018-095076-B-C22, and TIN2015-65316-P (‘Computación de Altas Prestaciones VII’), the Juan de la Cierva Incorporación Programme (FJCI-2015-2671 and IJC2019-04862-I for F. Anders), the Severo Ochoa Centre of Excellence Programme (SEV2015-0493), and MICIN/AEI/10.13039/501100011033 (and the European Union through European Regional Development Fund ‘A way of making Europe’) through grant RTI2018-095076-B-C21, the Institute of Cosmos Sciences University of Barcelona (ICCUB, Unidad de Excelencia ‘María de Maeztu’) through grant CEX2019-000918-M, the University of Barcelona’s official doctoral programme for the development of an R+D+i project through an Ajuts de Personal Investigador en Formació (APIF) grant, the Spanish Virtual Observatory through project AyA2017-84089, the Galician Regional Government, Xunta de Galicia, through grants ED431B-2021/36, ED481A-2019/155, and ED481A-2021/296, the Centro de Investigación en Tecnologías de la Información y las Comunicaciones (CITIC), funded by the Xunta de Galicia and the European Union (European Regional Development Fund – Galicia 2014-2020 Programme), through grant ED431G-2019/01, the Red Española de Supercomputación (RES) computer resources at MareNostrum, the Barcelona Supercomputing Centre - Centro Nacional de Supercomputación (BSC-CNS) through activities AECT-2017-2-0002, AECT-2017-3-0006, AECT-2018-1-0017, AECT-2018-2-0013, AECT-2018-3-0011, AECT-2019-1-0010, AECT-2019-2-0014, AECT-2019-3-0003, AECT-2020-1-0004, and DATA-2020-1-0010, the Departament d’Innovació, Universitats i Empresa de la Generalitat de Catalunya through grant 2014-SGR-1051 for project ‘Models de Programació i Entorns d’Execució Parallels’ (MPEXPAR), and Ramon y Cajal Fellowship RYC2018-025968-I funded by MICIN/AEI/10.13039/501100011033 and the European Science Foundation (‘Investing in your future’);
 - the Swedish National Space Agency (SNSA/Rymdstyrelsen);
 - the Swiss State Secretariat for Education, Research, and Innovation through the Swiss Activités Nationales Complémentaires and the Swiss National Science Foundation through an Eccellenza Professorial Fellowship (award PCEFP2_194638 for R. Anderson);
 - the United Kingdom Particle Physics and Astronomy Research Council (PPARC), the United Kingdom Science and Technology Facilities Council (STFC), and the United Kingdom Space Agency (UKSA) through the following grants to the University of Bristol, the University of Cambridge, the University of Edinburgh, the University of Leicester, the Mullard Space Sciences Laboratory of University College London, and the United Kingdom Rutherford Appleton Laboratory (RAL): PP/D006511/1, PP/D006546/1, PP/D006570/1, ST/I000852/1, ST/J005045/1, ST/K00056X/1, ST/K000209/1, ST/K000756/1, ST/L006561/1, ST/N000595/1, ST/N000641/1, ST/N000978/1, ST/N001117/1, ST/S000089/1, ST/S000976/1, ST/S000984/1, ST/S001123/1, ST/S001948/1, ST/S001980/1, ST/S002103/1, ST/V000969/1, ST/W002469/1, ST/W002493/1, ST/W002671/1, ST/W002809/1, and EP/V520342/1.
- The *Gaia* project and data processing have made use of:
- the Set of Identifications, Measurements, and Bibliography for Astronomical Data (SIMBAD, [Wenger et al. 2000](#)), the ‘Aladin sky atlas’ ([Bonnarel et al. 2000](#); [Boch & Fernique 2014](#)), and the Vizier catalogue access tool ([Ochsenbein et al. 2000](#)), all operated at the Centre de Données astronomiques de Strasbourg ([CDS](#));
 - the National Aeronautics and Space Administration (NASA) Astrophysics Data System ([ADS](#));
 - the SPace ENVironment Information System (SPENVIS), initiated by the Space Environment and Effects Section (TEC-EES) of ESA and developed by the Belgian Institute for Space Aeronomy (BIRA-IASB) under ESA contract through ESA’s General Support Technologies Programme (GSTP), administered by the BELgian federal Science Policy Office (BELSPO);
 - the software products [TOPCAT](#), [STIL](#), and [STILTS](#) ([Taylor 2005, 2006](#));
 - [Matplotlib](#) ([Hunter 2007](#));
 - [IPython](#) ([Pérez & Granger 2007](#));
 - [Astropy](#), a community-developed core Python package for Astronomy ([Astropy Collaboration et al. 2018](#));
 - [R](#) ([R Core Team 2013](#));

- Vaex (Breddels & Veljanoski 2018);
- the HIPPARCOS-2 catalogue (van Leeuwen 2007). The HIPPARCOS and *Tycho* catalogues were constructed under the responsibility of large scientific teams collaborating with ESA. The Consortia Leaders were Lennart Lindegren (Lund, Sweden: NDAC) and Jean Kovalevsky (Grasse, France: FAST), together responsible for the HIPPARCOS Catalogue; Erik Høg (Copenhagen, Denmark: TDAC) responsible for the *Tycho* Catalogue; and Catherine Turon (Meudon, France: INCA) responsible for the HIPPARCOS Input Catalogue (HIC);
- the *Tycho-2* catalogue (Høg et al. 2000), the construction of which was supported by the Velux Foundation of 1981 and the Danish Space Board;
- The *Tycho* double star catalogue (TDSC, Fabricius et al. 2002), based on observations made with the ESA HIPPARCOS astrometry satellite, as supported by the Danish Space Board and the United States Naval Observatory through their double-star programme;
- data products from the Two Micron All Sky Survey (2MASS, Skrutskie et al. 2006), which is a joint project of the University of Massachusetts and the Infrared Processing and Analysis Center (IPAC) / California Institute of Technology, funded by the National Aeronautics and Space Administration (NASA) and the National Science Foundation (NSF) of the USA;
- the ninth data release of the AAVSO Photometric All-Sky Survey (APASS, Henden et al. 2016), funded by the Robert Martin Ayers Sciences Fund;
- the first data release of the Pan-STARRS survey (Chambers et al. 2016; Magnier et al. 2020a; Waters et al. 2020; Magnier et al. 2020c,b; Flewelling et al. 2020). The Pan-STARRS1 Surveys (PS1) and the PS1 public science archive have been made possible through contributions by the Institute for Astronomy, the University of Hawaii, the Pan-STARRS Project Office, the Max-Planck Society and its participating institutes, the Max Planck Institute for Astronomy, Heidelberg and the Max Planck Institute for Extraterrestrial Physics, Garching, The Johns Hopkins University, Durham University, the University of Edinburgh, the Queen’s University Belfast, the Harvard-Smithsonian Center for Astrophysics, the Las Cumbres Observatory Global Telescope Network Incorporated, the National Central University of Taiwan, the Space Telescope Science Institute, the National Aeronautics and Space Administration (NASA) through grant NNX08AR22G issued through the Planetary Science Division of the NASA Science Mission Directorate, the National Science Foundation through grant AST-1238877, the University of Maryland, Eotvos Lorand University (ELTE), the Los Alamos National Laboratory, and the Gordon and Betty Moore Foundation;
- the second release of the Guide Star Catalogue (GSC2.3, Lasker et al. 2008). The Guide Star Catalogue II is a joint project of the Space Telescope Science Institute (STScI) and the Osservatorio Astrofisico di Torino (OATo). STScI is operated by the Association of Universities for Research in Astronomy (AURA), for the National Aeronautics and Space Administration (NASA) under contract NAS5-26555. OATo is operated by the Italian National Institute for Astrophysics (INAF). Additional support was provided by the European Southern Observatory (ESO), the Space Telescope European Coordinating Facility (STECF), the International GEMINI project, and the European Space Agency (ESA) Astrophysics Division (nowadays SCI-S);
- the eXtended, Large (XL) version of the catalogue of Positions and Proper Motions (PPM-XL, Roeser et al. 2010);
- data products from the Wide-field Infrared Survey Explorer (WISE), which is a joint project of the University of California, Los Angeles, and the Jet Propulsion Laboratory/California Institute of Technology, and NEOWISE, which is a project of the Jet Propulsion Laboratory/California Institute of Technology. WISE and NEOWISE are funded by the National Aeronautics and Space Administration (NASA);
- the first data release of the United States Naval Observatory (USNO) Robotic Astrometric Telescope (URAT-1, Zacharias et al. 2015);
- the fourth data release of the United States Naval Observatory (USNO) CCD Astrograph Catalogue (UCAC-4, Zacharias et al. 2013);
- the sixth and final data release of the Radial Velocity Experiment (RAVE DR6, Steinmetz et al. 2020a,b). Funding for RAVE has been provided by the Leibniz Institute for Astrophysics Potsdam (AIP), the Australian Astronomical Observatory, the Australian National University, the Australian Research Council, the French National Research Agency, the German Research Foundation (SPP 1177 and SFB 881), the European Research Council (ERC-StG 240271 Galactic), the Istituto Nazionale di Astrofisica at Padova, the Johns Hopkins University, the National Science Foundation of the USA (AST-0908326), the W.M. Keck foundation, the Macquarie University, the Netherlands Research School for Astronomy, the Natural Sciences and Engineering Research Council of Canada, the Slovenian Research Agency, the Swiss National Science Foundation, the Science & Technology Facilities Council of the UK, Opticon, Strasbourg Observatory, and the Universities of Basel, Groningen, Heidelberg, and Sydney. The RAVE website is at <https://www.rave-survey.org/>;
- the first data release of the Large sky Area Multi-Object Fibre Spectroscopic Telescope (LAMOST DR1, Luo et al. 2015);
- the K2 Ecliptic Plane Input Catalogue (EPIC, Huber et al. 2016);
- the ninth data release of the Sloan Digital Sky Survey (SDSS DR9, Ahn et al. 2012). Funding for SDSS-III has been provided by the Alfred P. Sloan Foundation, the Participating Institutions, the National Science Foundation, and the United States Department of Energy Office of Science. The SDSS-III website is <http://www.sdss3.org/>. SDSS-III is managed by the Astrophysical Research Consortium for the Participating Institutions of the SDSS-III Collaboration including the University of Arizona, the Brazilian Participation Group, Brookhaven National Laboratory, Carnegie Mellon University, University of Florida, the French Participation Group, the German Participation Group, Harvard University, the Instituto de Astrofísica de Canarias, the Michigan State/Notre Dame/JINA Participation Group, Johns Hopkins University, Lawrence Berkeley National Laboratory, Max Planck Institute for Astrophysics, Max Planck Institute for Extraterrestrial Physics, New Mexico State University, New York University, Ohio State University, Pennsylvania State University, University of Portsmouth, Princeton University, the Spanish Participation Group, University of Tokyo, University of Utah, Vanderbilt University, University of Virginia, University of Washington, and Yale University;
- the thirteenth release of the Sloan Digital Sky Survey (SDSS DR13, Albareti et al. 2017). Funding for SDSS-IV has been provided by the Alfred P. Sloan Foundation, the United States Department of Energy Office of Science, and the Participating Institutions. SDSS-IV acknowledges support and

resources from the Center for High-Performance Computing at the University of Utah. The SDSS web site is <https://www.sdss.org/>. SDSS-IV is managed by the Astrophysical Research Consortium for the Participating Institutions of the SDSS Collaboration including the Brazilian Participation Group, the Carnegie Institution for Science, Carnegie Mellon University, the Chilean Participation Group, the French Participation Group, Harvard-Smithsonian Center for Astrophysics, Instituto de Astrofísica de Canarias, The Johns Hopkins University, Kavli Institute for the Physics and Mathematics of the Universe (IPMU) / University of Tokyo, the Korean Participation Group, Lawrence Berkeley National Laboratory, Leibniz Institut für Astrophysik Potsdam (AIP), Max-Planck-Institut für Astronomie (MPIA Heidelberg), Max-Planck-Institut für Astrophysik (MPA Garching), Max-Planck-Institut für Extraterrestrische Physik (MPE), National Astronomical Observatories of China, New Mexico State University, New York University, University of Notre Dame, Observatório Nacional / MCTI, The Ohio State University, Pennsylvania State University, Shanghai Astronomical Observatory, United Kingdom Participation Group, Universidad Nacional Autónoma de México, University of Arizona, University of Colorado Boulder, University of Oxford, University of Portsmouth, University of Utah, University of Virginia, University of Washington, University of Wisconsin, Vanderbilt University, and Yale University;

- the second release of the SkyMapper catalogue (SkyMapper DR2, [Onken et al. 2019](#), Digital Object Identifier 10.25914/5ce60d31ce759). The national facility capability for SkyMapper has been funded through grant LE130100104 from the Australian Research Council (ARC) Linkage Infrastructure, Equipment, and Facilities (LIEF) programme, awarded to the University of Sydney, the Australian National University, Swinburne University of Technology, the University of Queensland, the University of Western Australia, the University of Melbourne, Curtin University of Technology, Monash University, and the Australian Astronomical Observatory. SkyMapper is owned and operated by The Australian National University’s Research School of Astronomy and Astrophysics. The survey data were processed and provided by the SkyMapper Team at the the Australian National University. The SkyMapper node of the All-Sky Virtual Observatory (ASVO) is hosted at the National Computational Infrastructure (NCI). Development and support the SkyMapper node of the ASVO has been funded in part by Astronomy Australia Limited (AAL) and the Australian Government through the Commonwealth’s Education Investment Fund (EIF) and National Collaborative Research Infrastructure Strategy (NCRIS), particularly the National eResearch Collaboration Tools and Resources (NeCTAR) and the Australian National Data Service Projects (ANDS);
- the *Gaia*-ESO Public Spectroscopic Survey (GES, [Gilmore et al. 2022](#); [Randich et al. 2022](#)). The *Gaia*-ESO Survey is based on data products from observations made with ESO Telescopes at the La Silla Paranal Observatory under programme ID 188.B-3002. Public data releases are available through the [ESO Science Portal](#). The project has received funding from the Leverhulme Trust (project RPG-2012-541), the European Research Council (project ERC-2012-AdG 320360-Gaia-ESO-MW), and the Istituto Nazionale di Astrofisica, INAF (2012: CRA 1.05.01.09.16; 2013: CRA 1.05.06.02.07).

ern Hemisphere (ESO) with the VLT Survey Telescope (VST), under ESO programmes 092.B-0165, 093.B-0236, 094.B-0181, 095.B-0046, 096.B-0162, 097.B-0304, 098.B-0030, 099.B-0034, 0100.B-0131, 0101.B-0156, 0102.B-0174, and 0103.B-0165; and (ii) the Liverpool Telescope, which is operated on the island of La Palma by Liverpool John Moores University in the Spanish Observatorio del Roque de los Muchachos of the Instituto de Astrofísica de Canarias with financial support from the United Kingdom Science and Technology Facilities Council, and (iii) telescopes of the Las Cumbres Observatory Global Telescope Network.

The GBOT programme uses observations collected at (i) the European Organisation for Astronomical Research in the South-